

Mineral Chemistry and Reaction Textures of Calc-silicate Rocks of the Lunavada Region, SAMB, NE Gujarat

Gayatri Akolkar* and M. A. Limaye

Department of Geology, Faculty of Science, The Maharaja Sayajirao University of Baroda, Vadodara - 390 002, India

*Email: akolkargayatri@gmail.com

ABSTRACT

Calc-silicate rocks occurring in and around Lunavada town belong to the Kadana Formation of the Lunavada Group of the Aravalli Supergroup. These rocks are embedded within pelitic schists in the form of sporadically distributed lensoidal bodies and are surrounded by quartzitic ridges. Rocks of the Kadana Formation and its surrounding area have experienced intrusive event named as 'Godhra granite' which occupy the SW part of this area. Some prominent field characteristics shown by these calc-silicates include fine to medium grained size, dark grey colour, unoriented/star shaped amphibole needles and maculose structure. These rocks have contact metamorphic textural features and the typical mineral assemblage viz., $Act + Di + Qtz + Ttn + Cal \pm Mc \pm Bt \pm Pl \pm Ep \pm Scp \pm Chl$ with minor proportion of apatite, zircon and opaques. EPMA studies revealed that the Ca-amphibole composition of these rocks ranges from magnesio-hornblende to actinolite whereas the clinopyroxene is salitic to diopsidic and the mica is found to be phlogopitic biotite. Certain prograde and retrograde reactions textures present within these rocks have been interpreted, for e.g. the development of diopside (salite) from ankeritic composition which is then retrogressed and actinolite appeared, prograde reaction leading to the formation of titanite from ilmenite and calcite and breakdown of scapolite into calcite and quartz with plagioclase lacking co-existence with these scapolites, indicating retrogression. Mineral assemblage and mineral chemistry data interpretation points towards the calcareous sandstone or marl as a probable protolith having impure calcareous composition, moreover, field characteristics and reaction textures observed give indication that the protolith might had passed through the contact metamorphic event to give rise to the present day calc-silicates.

INTRODUCTION

The calc-silicate rocks of the area under investigation belong to the Lunavada Group which is the second youngest Group of the Aravalli Supergroup and make a part of Southern Aravalli Mountain Belt (SAMB) in Gujarat. These rocks are of Meso-proterozoic age and represent the youngest formation of Lunavada Group known as 'Kadana Formation' (Iqbaluddin, 1989; Gupta et al. 1992, 1997). In the previous studies of this area greater attention was paid on the various aspects like lithostratigraphy, sedimentology and structural geology by Gupta and Mukherjee (1938), Iqbaluddin and Venkatramaiah (1976) and Mamtani (1998) as well as Mamtani et al. (1999a, 2000) respectively and very little is known about the genesis of the calc-silicates present here unlike the calc-silicates of neighbouring area present in the Champaner Group where these rocks have been studied in great details with respect to petrology by Das et al. (2009). The present paper contributes to petrography, mineral chemistry and mineral parageneses in terms of prograde and retrograde reaction textures of these rocks for the first time and on the basis of these

studies it will become possible to acquire the general idea regarding the protolith of these calc-silicates and the metamorphic events they had gone through.

GEOLOGICAL SETTING

The Lunavada Group occupies an area of 10,000 sq.km and covers NE part of Gujarat state partially and is having its extension in SW part of Rajasthan (Merh, 1995). As per the stratigraphy, only a part of Lunavada Group falls within the Gujarat state known as the Kadana Formation while remaining five formations of this Group occupy the areas of southern Rajasthan (Iqbaluddin, 1989). In this group, argillaceous as well as arenaceous metasediments with thin bands of calcareous rocks intercalated within them are found to occur, viz. phyllites, mica schists, chlorite schists, meta-siltstones, meta-semipelites, meta-protoquartzites with thin sheets of dolomitic limestone, petromict meta-conglomerate, manganiferous phyllite and phosphetic algal dolomite (Gupta et al., 1980, 1992). Study area under investigation lies in the SE part of Lunavada town between latitudes 23°00'-23°09' N and longitudes 73°35'-73°45' E (Fig.1). In this area only three major lithologies i.e. quartzites, pelitic schists and calc-silicate rocks have been encountered and the isolated lensoidal bodies of calc-silicates reside along with the pelitic schists in the planar areas which are surrounded by tightly folded quartzitic ridges. Impressions of regional scale folding events can be identified as F_1 , F_2 and F_3 within rocks present in and around Lunavada, formed on account of D_1 - D_3 deformational episodes where D_1 and D_2 are coaxial with NE-SW striking axial traces, whereas D_3 marks the NW-SE trend and is coeval with the granite emplacement (Mamtani et al., 2001; Mamtani et al., 2002; Mamtani and Greiling, 2005; Sen and Mamtani, 2006). Several NW-SE trending axial planar slippages have also been recorded with the last phase of deformation (Mamtani et al., 1999a; Joshi et al., 2016). 'Godhra Granite' which is intrusive into the Kadana Formation and surrounding area occurs at the SW part of the study area whereas younger extrusive basaltic rocks are exposed on the eastern margin of the study area (Gupta et al., 1980; 1995). These granites have Neoproterozoic age i.e. 955 ± 20 Ma (Gopalan et al., 1979). Calc-silicate rocks under study exhibit fine to medium grained size and dark grey colour. Development of unoriented/star shaped actinolite porphyroblasts can be observed within these rocks (Fig.2a). Maculose structure is also prominently developed over these rock surfaces (Fig.2b). Apart from it other features observed are compositional bandings as well as foliations, in rare cases (Fig.2c and 2d).

PETROGRAPHY

These rocks are characterized by prominent hornfelsic texture which is defined by unoriented actinolite needles and hence considered as hornfels (Bhaskar Rao, 1986). Apart from this, porphyro-poikiloblastic texture and the granoblastic polygonal groundmass composed of quartz and plagioclase feldspar in some samples are

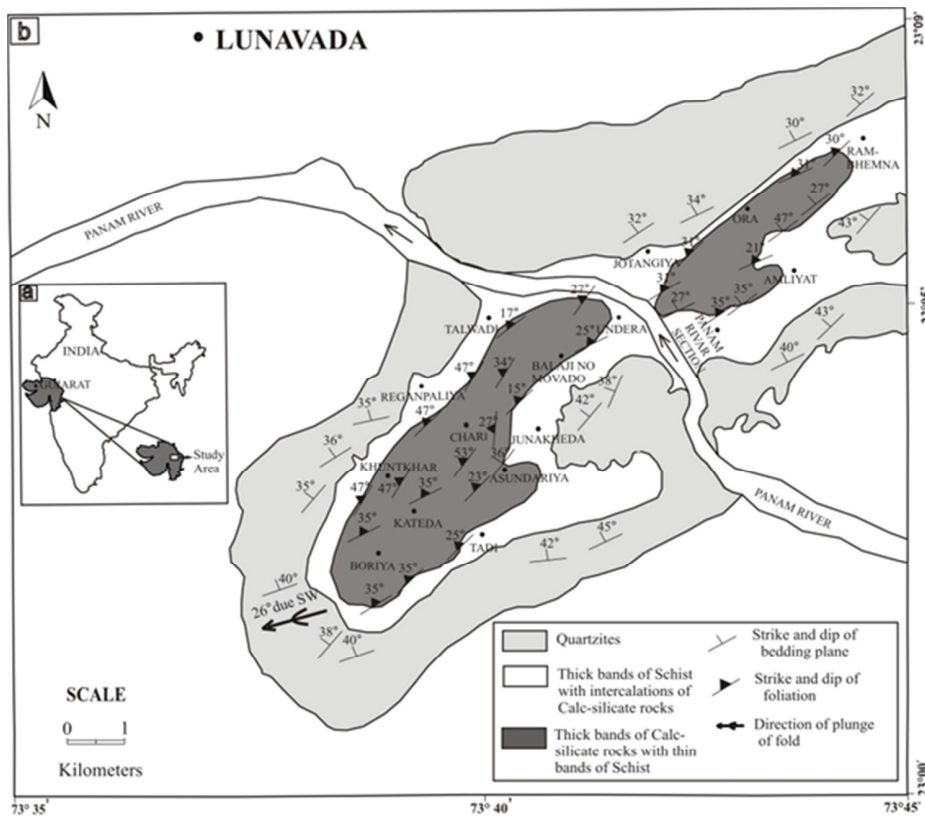


Fig.1. (a) Location map and (b) Geological map of the study area, (modified after Mamtani, 1998)

some minor textures observed in these rocks. The typical mineral assemblage of these calc-silicates is actinolite + diopside + quartz + titanite + calcite ± microcline ± biotite ± plagioclase feldspar ($An_{32} - An_{67}$) ± epidote ± scapolite ± chlorite along with minor proportion of apatite, zircon and opaques.

Although most of the actinolites are unoriented or star shaped,

rarely oriented actinolites can also be observed. They are strongly pleochroic with colourless to pale green pleochroism. Oriented actinolites are found to be comparatively slender and most of them are devoid of any inclusion. Inclusion trails of quartz or diopside when present in the actinolites of these rocks, show concordant relationship with the groundmass fabric and also the quartz inclusions exhibit sharp extinction suggesting post-tectonic growth of these porphyroblasts (Ghosh, 1993 and Passchier and Trouw, 2005). Simple twinning is shown by some actinolite grains. Apart from acicular or needle shape, rhombic to pseudo-hexagonal shaped actinolites are also seen to be developed due to their typical amphibole cleavage on (110). Diopside is subidioblastic, can be distinguished by its high relief, weak pleochroism and two distinct cleavages almost at 90° angle. It is enclosing dolomitic (or ankeritic) mass indicating its formation at the expense of latter (Fig.3a). Similarly, it makes most part of the groundmass in some samples and is present in the form of inclusions within actinolite porphyroblasts (Fig.3b). Titanite grains exhibit their characteristic wedge or spindle shape or sometimes distorted

shape and distinct relief. They can be seen to be closely associated with ilmenite and quartz (Fig.3c). Plagioclase feldspar ($An_{32} - An_{67}$) occurs as fine to medium-sized tabular, subidioblastic grains with 2-5% modal amount. Biotite can be seen along the margins of actinolite in the matrix of microcline frequently (Fig.3d). In some thin sections biotite laths are getting altered to chlorites.

Pleochroic haloes can also be seen within biotites. Anhydrous epidote grains are commonly associated with actinolites and they are almost non-pleochroic and exhibit higher order colours. Anhydrous to sub-hedral scapolite grains can be seen in the form of granular clusters and exhibit moderate relief with well developed cleavages and are found to be closely associated with calcite and quartz (Fig.3e). Rarely, myrmekitic texture can be seen in some rock samples developed due to the intergrowth of quartz in plagioclase feldspar (Fig.3f).

MINERAL CHEMISTRY

To know the mineral chemistry, the Electron Probe Micro Analysis (EPMA) was carried out for all important mineral phases present in these rocks with the help of CAMECA SXFive instrument at DST-SERB National Facility, Department of Geology (Center of Advanced Study), Institute of Science, Banaras Hindu University. Polished thin sections were coated with 20 nm thin layer of carbon for electron probe micro analyses using

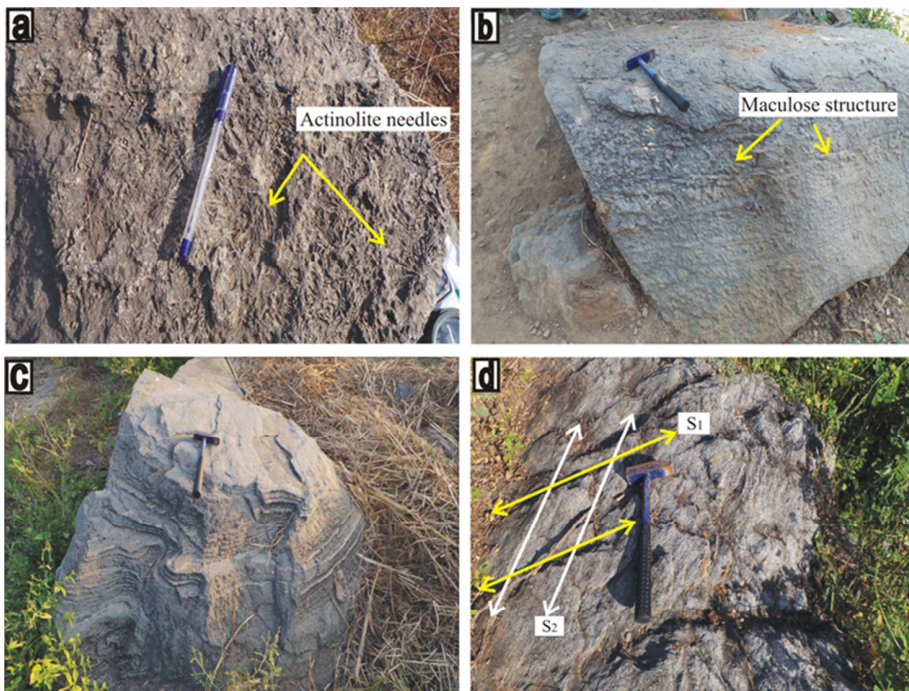


Fig.2. Field photographs showing (a) unoriented/star shaped actinolite needles on the surface of calc-silicate rocks, Loc. E of Jotangiya. (b) Maculose structure developed over the surface of calc-silicate rock, Loc. N of Amliyat (c) Compositional bandings within calc-silicates, Loc. N of Chari. (d) Foliated calc-silicate rock, (S_1 , S_2 foliations can be seen), Loc. Panam river section.

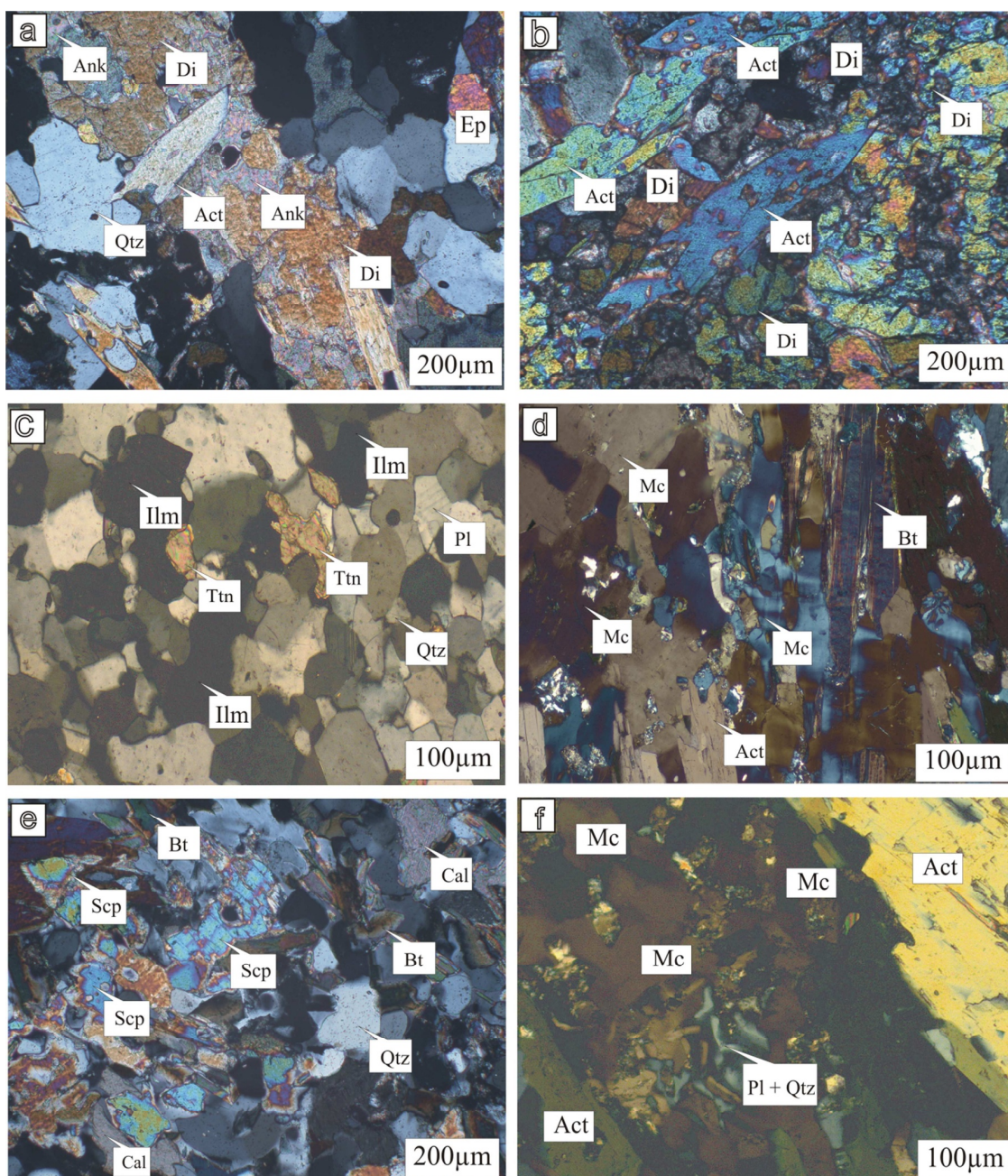


Fig.3. Photomicrographs of calc-silicate rocks in crossed polars showing (a) Salite nucleating from ankeritic composition. (b) Actinolites with numerous inclusions of associated diopside suggesting formation of actinolite at the expense of latter. (c) Replacement of ilmenite by titanite grains. (d) Retrogression of actinolite indicated by the formation of biotite along the actinolite margins in association with microcline. (e) Replacement of scapolite by calcite and quartz indicates retrogressed scapolite, here the presence of plagioclase is lacking. (f) Development of myrmekitic texture having close association of alkali feldspar (microcline).

LEICA-EM ACE200 instrument. The CAMECA SXFive instrument was operated by SXFive Software at a voltage of 15 kV and current 10 nA with a W source in the electron gun for generation of electron beam. Natural mineral standards were used for routine calibration and quantification. Representative microprobe analyses of major and important minerals present within these calc-silicate rocks are as follows:

Calcic-amphibole

All studied amphiboles can be classified as calcic amphiboles as per the nomenclature suggested by Leake (1978) and these calcic amphiboles correspond to the magnesio-hornblende to actinolite with $(Na+K)_A < 0.5$ apfu, $Ti < 0.5$ apfu. (Table II, Leake et al., 1997), (Fig.4a). Those amphiboles which plot in the magnesio-hornblendes field

(Fig.4c) contain 7.1-7.5 apfu Si, 0.9-1.3 apfu Al^{tot} , and $(Mg / Mg+Fe^{2+})$ values between 0.67 to 0.78 and those with actinolitic composition contain 7.5 to 7.9 apfu Si, 0.26-0.76. apfu Al^{tot} , and $(Mg / Mg+Fe^{2+})$ values between 0.68 to 0.79. Manganese and Ti are present in amounts from 0.00 to 0.07 apfu (Table 1).

Clinopyroxene

Clinopyroxene (Cpx), is essentially a diopside-hedenbergite solid solution ($Wo_{47-53}, En_{34-39}, Fs_{10-15}$). The composition is salitic to diopsidic (Table 1) with X_{Mg} ranging between 0.76 and 0.82. The Al is both tetrahedrally and octahedrally co-ordinated. Most of the analysed clinopyroxenes fall in the salitic field in the Ca-Mg-Fe triangular plot (Fig.4b). Clinopyroxenes contain 1.79- 2.00 apfu of Si, 0.02-0.2 apfu of Al^{tot} , Fe^{3+} 0.00-0.08 apfu. Na ranges from 0.01-

Table 1. Representative electron microprobe analyses of calcic-amphibole and clinopyroxene

Rock no.	Calcic-amphibole				Rock no.	Clinopyroxene		
	PRS-10	RGP-13	BR-10	ASN-17		PRS-10	BR-10	ORA-6
SiO ₂	51.26	50.02	53.86	48.80	SiO ₂	54.71	52.41	52.01
TiO ₂	0.10	0.09	0.02	0.33	TiO ₂	0.03	0.03	0.01
Al ₂ O ₃	3.56	4.82	1.55	7.96	Al ₂ O ₃	25.56	50.74	0.64
FeO	8.59	11.11	9.45	12.14	Cr ₂ O ₃	0.92	0.04	1.19
MnO	0.59	0.35	0.38	0.51	FeO	4.37	6.60	7.29
MgO	16.93	15.46	17.29	13.65	MnO	0.62	0.66	0.22
CaO	14.33	12.65	12.83	11.87	MgO	10.44	13.87	13.44
Na ₂ O	0.31	0.51	0.09	0.84	CaO	18.53	24.81	24.02
K ₂ O	0.24	0.38	0.07	1.23	Na ₂ O	0.16	0.20	0.18
Total	95.95	95.44	95.57	97.35	K ₂ O	4.23	0.001	0.062
					Total	99.62	99.41	99.09
Ions on the basis of 23(O)					Ions on the basis of 6(O)			
Si	7.37	7.39	7.79	7.12	Si	1.79	2.01	1.95
Ti	0.01	0.01	0.00	0.03	Ti	0.006	0.0005	0.0004
Al	0.60	0.84	0.26	1.37	Al	0.21	0.03	0.02
Fe ²⁺	1.03	1.37	1.14	1.48	Cr	0.13	0.05	0.03
Mn	0.07	0.04	0.04	0.06	Fe ²⁺	0.14	0.19	0.22
Mg	3.63	3.40	3.73	2.97	Mn	0.02	0.02	0.007
Ca	2.20	2.00	1.99	1.85	Mg	0.66	0.64	0.75
Na	0.08	0.14	0.02	0.23	Ca	0.98	0.96	0.96
K	0.04	0.07	0.01	0.22	Na	0.02	0.05	0.01
					K	0.003	0.008	0.003
% Mg/(Mg + Fe)	0.78	0.71	0.76	0.67	Mg/(Mg + Fe ^{tot})	0.82	0.76	0.77
					Pyx. components			
					Wo	53.68	51.24	49.11
					En	36.14	34.36	38.23
					Fs	9.08	11.65	11.96

0.05 apfu. Manganese varies from 0.007 and 0.02 apfu. K, Cr and Ti are below detection limit.

Titanite

Titanite contains 0.95 -1.02 apfu Ca, 0.84-0.90 apfu Ti, 0.15-0.29 apfu Al. Mg is below detection limit. A typical titanite has the formula Ca_{1.02}(Ti_{0.90}Al_{0.15}Fe_{0.01})Si_{0.96}(F_{0.07}Cl_{0.003}). Na, Mn, K and Ba were measured in amounts 0.00-0.57 wt % oxide concentrations (Table 2). Low analytical totals in the range of 92.7-98.3% , including all Fe calculated as Fe₂O₃ , suggest the presence of OH⁻ and/or F⁻ to maintain the charge balance during the coupled substitution reaction: Ti⁴⁺ + O²⁻ = Al³⁺ + F⁻ (Rene, 2008; Fukai, 2013).

Biotite

Biotite has a variable Ti content ranging from 1.68 to 2.14 wt %. The Ti content of biotite present in calc-silicates lying closer to the granitic intrusion is higher than those which are away from it on account of increase in temperature. Their X_{Mg} composition range is between 0.60 to 0.66 (Table 2). On the Al vs. Fe/(Fe + Mg) diagram of Deer et al. (1992) biotites of these calc-silicate rocks lie in the biotite zone but very near to phlogopite boundary (Fig.4c) with their (Fe/Mg+ Fe) ratio ranging from (0.33-0.37 apfu).

Scapolite

Scapolites of these rocks are Cl-absent calcic-rich meionites. Their Ca/(Ca+Na+K) ratios vary between 0.89 and 0.93. SO₃ and F contents are below detection limit. K₂O values are very low (0.1-0.2 wt %). The meionite component varies from 89.7 to 92.8 % (Table 2).

REACTION TEXTURES

Petrography revealed certain reaction textures which help to

understand the parageneses of various minerals present in these rocks and can be shown by following reactions:

Salite forming reaction

Textural evidence of progressive metamorphism can be shown with the help of reaction texture viz. enclosed dolomite (or ankerite) by salite in the matrix of quartz. Thus it can be stated that the salite is getting formed at the expense of former. Since the salite is Fe rich variety of diopside, the carbonate phase on account of which it is getting produced must be ankerite i.e Fe rich carbonate (Fig.3a). Thus the formation of salite can be given by following reaction (Winter, 2001)



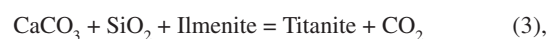
Actinolite forming reaction

Actinolite porphyroblasts show numerous inclusions of salite thereby indicating their formation at the expense of latter (Fig.3b). This is a retrograde reaction and is given as follows:



Titanite forming reaction

Titanite grains within these calc-silicates are found to be closely associated with ilmenite in the matrix of quartz + calcite (Fig.3c). The probable reaction leading to their formation is:



which is a prograde reaction.

Biotite forming reaction

In some of the specimens of calc-silicate rocks, biotite laths can be observed to be nucleating along the margins of actinolite needles

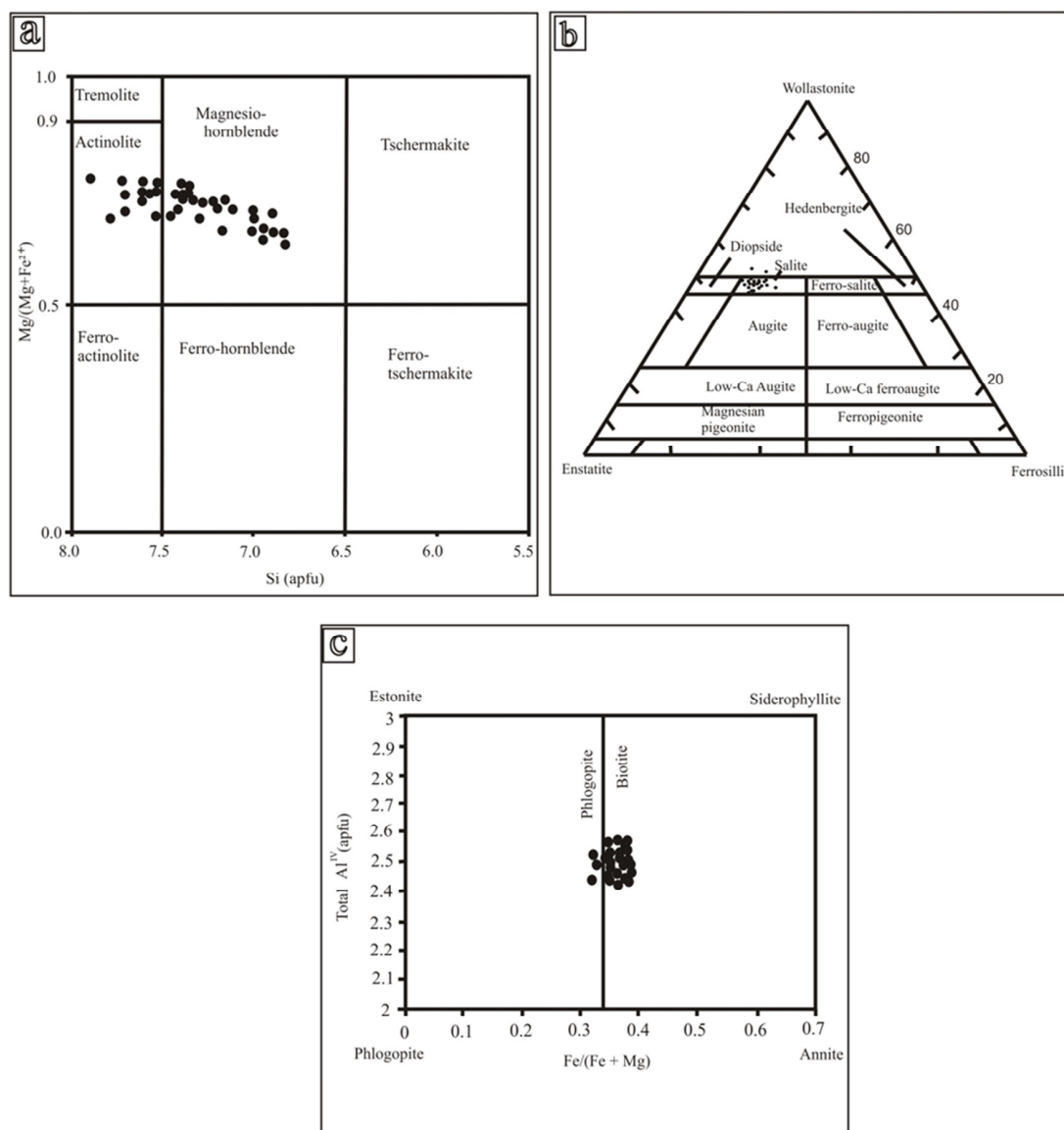
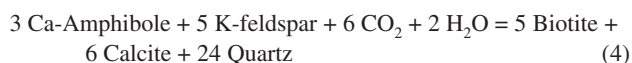


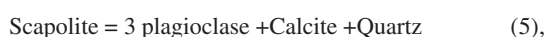
Fig.4. (a) Chemical composition of calcic-amphibole present in these rocks. Classification scheme (after Leake et al.1997). (b) Ca-Mg-Fe triangular plot showing clinopyroxene composition. (c) Mica composition ranges from biotite to phlogopite. Classification scheme (after Deer et al.1992).

which are associated with microcline (Fig.3d). This indicates following reaction,



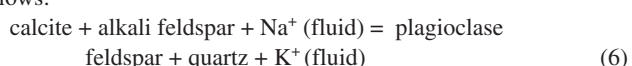
Scapolite forming reaction

Occurrence of scapolite within these calc-silicate rocks is limited to the narrow zone around granitic pluton. Retrogressed scapolite can be seen, as it is getting replaced by the calcite and quartz and the plagioclase is not associated with these scapolites (Fig.3e). This is considered as a vapour absent reaction and is given as follows:



(Satish-Kumar et al., 1995)

At places within these rocks, it has been found that the myrmekitic intergrowth of plagioclase feldspar and quartz is closely associated with alkali feldspar. This implies a fluid induced metasomatic retrograde reaction (Sameera et al., 2015), (Fig.3f). The reaction is as follows:



DISCUSSION AND CONCLUSIONS

The kind of mineral assemblage and textures observed in these rocks are typical of calc-silicate hornfels. The major minerals like Ca-amphibole and calcic-pyroxene present in these rocks are rich in both Mg and Fe, although Mg > Fe, i.e amphibole is actinolitic and pyroxene is salitic in composition. This is reflected from the classification diagram (see Fig.4a) and for clinopyroxene by Ca-Mg-Fe triangular plot (Fig.4b). Mica is a phlogopitic biotite. In the rock samples lying close to the granitic pluton occurrence of diopside (salite) has been noticed which indicates moderate to high temperature conditions whereas the appearance of scapolite is seen only within those samples lying very close to the pluton. These two minerals are then retrogressed which is shown by reaction textures present in these rocks. Retrogression by co-existing clinopyroxene and amphibole is also reported within the calc-granulites of Hammerhead syncline from Southern Sandmata Complex, NW India (Purohit et al., 2015). Effect of increased temperature due to nearby granitic pluton has led to the development of maculose structure over these rock surfaces. Typical contact metamorphism, viz. hornfelsic, porphyro-poikiloblastic texture and granoblastic polygonal groundmass (Winter, 2001) are typical of these calc-silicates also. Similarly, according to Deer et al. (1985)

Table 2. Representative electron microprobe analyses of titanite, biotite and scapolite

Titanite				Biotite				Scapolite		
Rock no.	PRS-10	ASN-17	ORA-6	Rock no.	PRS-10	ASN-17	BR-10	Rock no.	BR-10/34	BR-10/35
SiO ₂	26.66	29.23	29.96	SiO ₂	34.04	37.03	37.22	SiO ₂	42.44	44.81
TiO ₂	33.33	36.86	37.81	TiO ₂	1.68	1.70	2.14	Al ₂ O ₃	20.37	22.90
Al ₂ O ₃	2.06	1.74	1.89	Al ₂ O ₃	16.59	16.00	15.86	FeO	0.34	0.25
Fe ₂ O ₃	0.56	0.49	0.37	FeO	15.31	16.48	13.97	MnO	0.1	0.17
MnO	0.02	0.00	0.07	MnO	0.34	0.18	0.31	CaO ₂	2.89	23.36
CaO	25.74	29.17	29.26	MgO	16.52	14.22	14.54	Na ₂ O	2.31	1.99
Na ₂ O	0.43	0.06	0.00	CaO	0.05	0.00	0.00	K ₂ O	0.20	0.1
K ₂ O	0.16	10.07	0.02	Na ₂ O	0.09	0.09	0.01	P ₂ O ₅	0.48	0.39
Cr ₂ O ₃	7.01	70.66	0.06	K ₂ O	5.39	9.79	9.95			
P ₂ O ₅	0.48	0.60	0.53							
BaO	0.33	0.0003	0.26							
F	0.00	0.72	0.34							
Total	96.96	100.44	100.59	Total	90.01	95.49	94.00	Total	90.99	93.97
Ions on the basis of 5(O)				Ions on the basis of 22(O)				Ions on the basis of 12 (Si, Al)		
Si	0.91	0.95	1.02	Si	5.30	5.56	5.62	Si	6.46	6.81
Ti	0.86	0.90	0.84	Al ^{IV}	2.69	2.43	2.37	Al	2.78	3.07
Al	0.18	0.15	0.28	Al ^{VI}	0.34	0.39	0.44	Fe ²⁺	0.02	0.01
Fe ³⁺	0.01	0.01	0.009	Ti	0.19	0.19	0.24	Mn	0.006	0.01
Mn	0.0006	0.00	0.001	Fe ²⁺	1.99	2.07	1.76	Ca	1.78	1.9
Ca	0.95	1.02	0.95	Mn	0.04	0.02	0.04	Na	0.19	0.14
Na	0.02	0.003	0.00	Mg	3.83	3.18	3.27	K	0.01	0.00
K	0.007	0.003	0.03	Ca	0.009	0.00	0.00	P	0.03	40.02
P	0.04	0.05	0.04	Na	0.02	0.02	0.003			
Ba	0.004	0.00	0.005	K	1.07	1.87	1.91			
F	0.00	0.07	0.05	X _{Mg}	0.66	0.60	0.65			
								Mol.% Meionite	89.67	92.77

more magnesium rich varieties of calcic-pyroxenes like diopside are essential constituents of contact metamorphism of calcium-rich sediments. Formation of calc-silicate hornfels on account of contact metamorphism of impure carbonates due to granitic intrusion (Godhra granite) leading to the development of minerals like diopside in these rocks has been observed by Das et al. (2009) in Champaner Group also. All these observations indicate the effect of contact metamorphism of Ca-rich sediments. Mineral chemistry of mineral assemblage reveals the presence of Fe rich Ca-amphibole, Fe rich Ca-pyroxene as well as moderate amount of biotite. This implies that impure calcareous sediments like calcareous sandstone/marl as probable protolith that has undergone contact metamorphism resulting in the formation of calc-silicate rocks of the area.

Acknowledgements: The authors are grateful to Prof. H. Kataria, Dean, Faculty of Science and I/C Head, Department of Geology, The M. S. University of Baroda, Vadodara for providing necessary facilities. The first author is also thankful to the DST-Woman scientist (WOS-A) project, for providing funding to carry out this work. First author is also thankful to Prof. L.S. Chamyal for his constant encouragement. We are indebted to two anonymous reviewers for their constructive comments and suggestions which improved the manuscript considerably. Authors thankfully acknowledge the help rendered by Prof. N.V. Chalapathi Rao and Dr. Dinesh Pandit, Banaras Hindu University, Varanasi, for carrying out EPMA analyses.

References

Bhaskar Rao, B. (1986) Metamorphic petrology. CRC Press, 182p.
 Das, S., Singh, P.K. and Srikarni, C. (2009) A preliminary study of thermal metamorphism in the Champaner Group of rocks in Panchmahals and

Vadodara districts of Gujarat. Indian Jour. Geosci., v.63(4), pp.373-382.
 Deer, W. A., Howie, R. A. and Zussman, J. (1985) An Introduction to the Rock Forming Minerals, Longman, London, 15th edition, 528p.
 Deer, W. A., Howie, R. A. and Zussman, J. (1992) An Introduction to the Rock Forming Minerals, Longman, London, 2nd edition, 696p.
 Fukai, I. (2013) Metamorphic and geochemical signatures of Calc-silicate gneisses from the Sawtooth metamorphic complex, Idaho, USA: Implications for the crustal evolution in the western north America. (Unpublished) Dissertation thesis.
 Ghosh, S.K. (1993) Structural Geology: Fundamentals and Developments. Pergamon Press, UK, 597p.
 Gopalan, K., Trivedi, J.R., Merh, S.S., Patel, P.P. and Patel, S.G. (1979) Rb-Sr age of Godhra and related granites, Gujarat (India). Proc. Indian Acad. Sci., Earth Planet. Sci., v.88A, pp.7-17.
 Gupta, B.C. and Mukherjee, P.N. (1938) Geology of Gujarat and Southern Rajputana. Rec. Geol. Surv. India, v.73, pp.163-208.
 Gupta, S.N., Arora, Y.K., Mathur, R.K., Iqbaluddin, B.P., Sahai, T.N. and Sharma, S.B. (1995) Geological Map of the Precambrians of the Aravalli Region, Southern Rajasthan and Northeastern Gujarat, India. Geol. Surv. India Publ., Hyderabad.
 Gupta, S.N., Arora, Y.K., Mathur, R.K., Iqbaluddin, B.P., Sahai, T.N. and Sharma, S.B. (1980) Lithostratigraphic Map of Aravalli Region, Southern Rajasthan and North Eastern Gujarat. Geol. Surv. India Publ., Hyderabad.
 Gupta, S.N., Arora, Y.K., Mathur, R.K., Iqbaluddin, B.P., Sahai, T.N. and Sharma, S.B. (1997) The Precambrian geology of the Aravalli region, Southern Rajasthan and Northeastern Gujarat. Mem. Geol. Surv. India, v.123, pp.58-65.
 Gupta, S.N., Mathur, R.K. and Arora, Y.K. (1992) Lithostratigraphy of Proterozoic rocks of Rajasthan and Gujarat. A Review, Rec. Geol. Surv. India. v.115, pp. 63-85.
 Iqbaluddin and Venkataramaiah, T. (1976) Photogeological mapping with selective checks in parts of Kadana Reservoir area, Panchmahal district, Gujarat. Rep. (Unpubl.) Geol. Surv. India (F.S.1975-76)

- Iqbaluddin, B.P. (1989) Geology of Kadana Reservoir Area, Panchmahals District, Gujarat and Banswara and Dungarpur districts, Rajasthan. Mem. Geol. Surv. India, v.121, pp.84.
- Joshi, A.U., Limaye, M. A. and Deota, B. S. (2016) Microstructural indicators of post-deformational brittle-ductile shear zones, Lunawada region, Southern Aravalli Mountain Belt, Gujarat, India. Jour. M.S.U.S.T, v.51(1), pp.19-27.
- Leake, B.E. (1978) Nomenclature of amphiboles. Amer. Mineral., v.63, pp.1023-1052.
- Leake, B.E., Woolley, A.R., Birch, W.D., Gilbert, M.C., Grice, J.D., Hawthorne, F.C., Kato, A., Kisch, H.J., Krivovichev, V.G., Linthout, K., Laird, J., Mandarino, J., Maresch, W.V., Nickel, E.H., Rock, N.M.S., Schumacher, J.C., Smith, D.C., Stephenson, N.C.N., Ungaretti, L., Whittaker, E.J.W. and Youzhi, G. (1997) Nomenclature of amphiboles - Report of the subcommittee on amphiboles of the International Mineralogical Association Commission on New Minerals and Mineral Names. European Jour. Mineral., v.9, pp.623-651.
- Mamtani, M. A., Karmakar I. B. and Merh, S.S. (2002) Evidence of Polyphase Deformation in Gneissic Rocks Around Devgadhi Bariya: Implications for Evolution of Godhra Granite in the Southern Aravalli Region (India) Gondwana Res., v.5(2), pp.401 -408.
- Mamtani, M.A. (1998) Deformational mechanisms of the Lunavada Pre-Cambrian rocks, Panchmahal district, Gujarat. Unpublished Ph.D.thesis, M.S. University of Baroda (India). pp.268.
- Mamtani, M.A. and Greiling, R.O. (2005) Granite emplacement and its relation with regional deformation in the Aravalli Mountain Belt (India)-inferences from magnetic fabric. Jour. Struct. Geol., v.27, pp.2008-2029.
- Mamtani, M.A., Greiling, R.O., Karanth, R.V. and Merh, S.S. (1999a) Orogenic deformation and its relation with AMS fabric - an Example from the Southern Aravalli Mountain Belt, India. In: Radhakrishna, T. and Piper, J.D. (Eds.), The Indian Subcontinent and Gondwana: A Palaeomagnetic and Rock Magnetic Perspective. Mem. Geol. Soc. India, no.44, pp.9-24.
- Mamtani, M.A., Karanth, R.V., Merh, S.S. and Greiling, R.O. (2000) Tectonic evolution of the Southern part of Aravalli Mountain Belt and its environs-possible causes and time constraints. Gondwana Res., v.3, pp.175-187.
- Mamtani, M.A., Merh, S.S., Karanth, R.V. and Greiling, R.O. (2001) Time relationship between metamorphism and deformation in the Proterozoic rocks of Lunavada region, southern Aravalli Mountain Belt (India) - a microstructural study. Jour. Asian Earth Sci., v.19, pp.195-205.
- Merh, S.S. (1995) Geology of Gujarat. Geological Society of India, Bangalore, 224p.
- Passchier, C.W. and Trouw, R.A.J. (2005) Microtectonics. Springer-Verlag, Heidelberg, 366p.
- Purohit, R., Papinaeu, D., Mehata, P., Fogel, M. and Dharma Rao, C.V. (2015) Study of Calc-Silicate Rocks of Hammer-Head Syncline from Southern Sandmata Complex, Northwestern India: Implications on Existence of an Archaean Protolith. Jour. Geol. Soc. India, v.85, pp.215-231.
- Rene, M. (2008) Titanite-ilmenite-magnetite phase relations in amphibolites of the Chynov area (Bohemian massif, Czech republic). Acta Geodyn. Geomater. v.5(3)151, pp.239-246.
- Sameera, K.A.G. and Perera, L.R.K. (2015) Petrological study of calc-silicate granulites in the Southern Highland Complex of Sri Lanka. Jour. Geol. Soc. Sri Lanka, v.17, pp.87-100 J.W. Herath Felicitation. Volume 87.
- Satish-Kumar, M., Santosh, M. and Yoshida, M. (1995) Reaction textures in Calc-Silicates as guides to the pressure - temperature - fluid History of granulite facies terrains in East Gondwana. Jour. Geosci., v.38, Act. 5, pp.89-114.
- Sen, K. and Mamtani, M.A. (2006) Magnetic fabric, shape preferred orientation and regional strain in granitic rocks. Jour. Struct. Geol., v.28, pp.1870-1882.
- Winter, J. D. (2001) An Introduction to Igneous and Metamorphic Petrology, Prentice Hall, Upper Saddle River, NJ, 796p.

(Received: 2 March 2019; Revised form accepted: 25 September 2020)



Geochemistry of calc-silicate rocks around Lunavada region, NE Gujarat: Implications for their protolith, provenance and tectonic setting

GAYATRI N AKOLKAR and MANOJ A LIMAYE*

Department of Geology, Faculty of Science, The Maharaja Sayajirao University of Baroda, Vadodara, Gujarat 390 002, India.

*Corresponding author. e-mail: manoj_geol@rediffmail.com

MS received 18 October 2019; revised 13 May 2020; accepted 19 June 2020

In this work, the calc-silicate rocks affiliated to the 'Kadana Formation', a youngest formation of the Lunavada Group have been investigated. These rocks are found to be embedded within associated rock types, viz., quartzites and metapelites in the form of isolated lensoidal bodies. Contact metamorphic textures and the typical mineral assemblage, viz., Act + Di + Cal + Qtz + Ttn ± Mc ± Pl ± Bt ± Ep ± Scp ± Chl with minor proportion of apatite, zircon and opaques can be observed in these calc-silicates. Major oxides, trace and rare earth elements were analysed to investigate the protolith type, provenance and tectonic setting of these rocks. Protolith must be calcareous sandstone with varied proportion of clay and deposited in shallow water environment as revealed by CaO, Al₂O₃ and FeO+MgO and Al–Zr–Ti ternary diagram, respectively. Low to moderate weathering of source rocks has been indicated by A–CN–K ternary diagram. Th/Sc vs. Zr/Sc and Th/Co vs. La/Sc plots confirm the continental source with felsic nature for these rocks and the calc-silicate samples fall within the active continental margin region of Sc–Th–Zr/10 diagram which also justify the kind of provenance for primary sediments.

Keywords. Calc-silicate rocks; Lunavada; Kadana; geochemistry; protolith; tectonic setting.

1. Introduction

Calc-silicate rocks are the type of metamorphic rocks primarily composed of calc-silicate minerals and contain less than 5% volume of carbonate minerals, i.e., calcite and/or aragonite and/or dolomite, as per the 'subcommission on the systematics of metamorphic rocks' (SCMR) classification scheme. The calc-silicates being investigated here belong to the Lunavada Group which is a second youngest group of the Aravalli Supergroup comprising an extension of the Southern Aravalli Mountain Belt (SAMB), which occupies the NE part of the Gujarat state. These rocks comprise youngest formation of Lunavada Group known as

Kadana Formation having Meso-proterozoic age (Iqbaluddin 1989; Gupta *et al.* 1992, 1997). The area around Lunavada has been variously investigated on the basis of their lithological (Gupta and Mukherjee 1938), sedimentological (Iqbaluddin and Venkataramaiah 1976) and structural (Mamtani *et al.* 1999, 2000) aspects. However, the calc-silicate rocks did not receive much attention. Therefore, present paper makes a maiden attempt to characterize this rock based on its major, trace and rare earth elements geochemistry. These data have been used to constrain the protolith characteristic and investigate the depositional environment, weathering history, provenance and tectonic setting. Understanding these aspects is of utmost

Lunavada terrain, whereas, garnet appears towards the southern part, indicating increase in the grade of metamorphism from greenschist to lower amphibolite facies from north to south (Mamtani 1998; Mamtani *et al.* 2001). ‘Godhra Granite’, which is intrusive to the Kadana Formation and the surrounding area, occurs towards the SW part of the study area whereas, the younger extrusive basaltic rocks are exposed on the eastern margin of the area (Gupta *et al.* 1980, 1995). The granites have shown Neoproterozoic age, i.e., 955 ± 20 Ma (Gopalan *et al.* 1979). The calc-silicate rocks exhibit fine to medium grained texture and light to dark grey colour. Characteristic features seen on the surfaces of these rocks include star shaped or unoriented actinolite needles (figure 2a) as well as the maculose structure developed on account of increased temperature due to intrusion of granites in close proximity to these rocks (figure 2b). Apart from this, minor features observed within these rocks are the compositional bandings, discordant granite-pegmatite veins and marginal orientation of actinolite needles in the calc-silicates lying in contact with adjacent

quartzite-metapelite intercalations (Akolkar *et al.* 2018).

3. Petrography

These rocks are characterized by the prominent granofelsic/hornfelsic texture which is defined by orientation of actinolite needles (Bhaskar Rao 1986; figure 2c). Apart from this, porphyro-poikiloblastic texture and the granoblastic polygonal groundmass can be observed as the minor textures. Groundmass is composed of quartz and microcline in some samples. These calc-silicate rocks possess a typical mineral assemblage as actinolite + diopside + quartz + titanite + calcite \pm microcline \pm biotite \pm plagioclase feldspar (An_{32} – An_{67}) \pm epidote \pm scapolite \pm chlorite along with minor apatite, zircon and opaques.

Although most of the actinolites are unoriented or star shaped, oriented actinolites can also be observed in rare cases. Due to their cleavage on (110), sometimes they assume rhombic or pseudo-hexagonal shape. Colourless to pale green pleochroism and simple twinning is shown by actinolite grains. Diopside is subidioblastic and

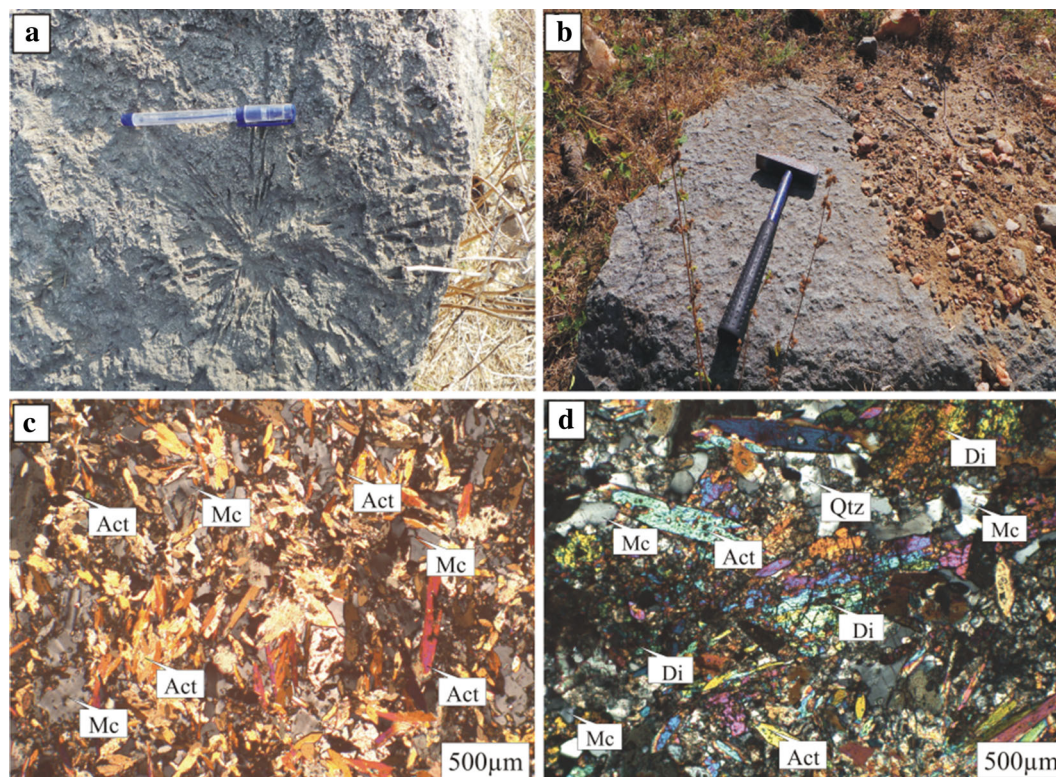


Figure 2. (a) Field photographs showing unoriented/star-shaped actinolite needles on the surface of calc-silicate rocks. Location Jotangiya. (b) Maculose structure developed over the surface of calc-silicate rock. Location Balaji no muvada. (c) Photomicrographs of calc-silicate rocks in crossed polars showing hornfelsic texture generated on account of disoriented actinolite needles. (d) Diopside can be seen in association with actinolite, microcline and quartz, formation of actinolite at the expense of diopside is indicated.

Table 1. Major (wt.%), trace and rare-earth elements (ppm) analyses of the representative calc-silicate rock samples of Lunavada area.

Sample no.	GCSL-1	GCSL-2	GCSL-3	GCSL-4	GCSL-5	GCSL-6
Lat.	23°5'48.9''	23°5'11.3''	23°04'56.9''	23°04'51.2''	23°03'30.1''	23°03'31.1''
Long.	73°43'17.8''	73°43'0.1''	73°42'27.6''	73°42'14.2''	73°40'11.5''	73°40'20.5''
SiO ₂	58.98	58.51	51.36	52.66	64.87	56.97
Al ₂ O ₃	13.15	12.13	8.46	9.18	7.82	8.46
Fe ₂ O ₃	5.79	6.05	6.69	5.89	4.12	5.88
MnO	0.13	0.19	0.37	0.35	0.25	0.27
MgO	7.27	8.43	15.59	13.39	5.99	11.47
CaO	6.76	7.18	13.50	12.99	12.72	10.11
Na ₂ O	1.31	0.80	0.80	0.93	0.28	0.81
K ₂ O	3.02	3.51	1.80	1.95	0.29	2.81
TiO ₂	0.79	0.82	0.51	0.58	0.84	0.57
P ₂ O ₅	0.24	0.16	0.24	0.16	0.24	0.17
LOI	0.71	0.54	0.44	0.48	0.62	0.63
Sum	98.15	98.32	99.76	98.56	98.04	98.15
Sc	8.0	9.1	9.2	7.5	11.0	8.4
V	49	60	67	35	74	66
Cr	41	73	43	65	56	52
Co	15.4	20.5	24.4	18.4	18.9	22.0
Ni	24.5	33.5	27.3	28.6	28.3	30.4
Cu	11.4	18.4	10.8	14.5	13.1	13.1
Zn	61	89	91	61	59	74
Ga	50.2	44.4	34.3	27.6	43.8	36.5
Rb	946.1	1332.2	603.6	101.4	762.4	636.3
Sr	144.8	124.8	131.0	206.3	167.5	101.6
Y	43.0	34.9	27.8	57.9	36.5	30.6
Zr	465.9	299.4	201.7	467.8	292.6	343.6
Nb	22.0	23.1	17.1	29.8	19.0	23.3
Cs	6.68	9.45	5.61	0.50	7.08	1.99
Ba	1378	1820	1115	156	1791	1714
La	46.1	29.7	23.7	60.4	30.3	22.1
Ce	95.9	61.0	48.7	126.2	69.6	46.0
Pr	10.2	6.5	5.4	13.6	6.9	4.9
Nd	40.3	25.7	22.1	53.9	27.4	20.0
Sm	8.3	5.4	4.8	11.1	5.9	4.3
Eu	1.5	1.0	0.9	1.7	1.1	0.8
Gd	6.7	4.7	4.1	8.9	5.0	3.9
Tb	1.1	0.8	0.7	1.5	0.9	0.7
Dy	7.6	5.9	4.9	9.9	6.4	5.3
Ho	1.6	1.3	1.1	2.1	1.4	1.1
Er	4.4	3.6	2.9	5.6	3.9	3.2
Tm	0.6	0.5	0.4	0.8	0.6	0.5
Yb	4.2	3.7	2.8	5.2	3.9	3.2
Lu	0.6	0.5	0.4	0.7	0.5	0.5
Hf	14.7	9.8	7.0	15.0	9.8	11.3
Ta	1.0	1.2	0.8	1.4	1.1	1.0
Pb	23.7	19.6	19.0	29.1	16.5	20.8
Th	47.8	41.8	27.1	66.5	33.6	35.9
U	2.2	1.9	1.3	3.0	1.4	1.6
(La/Sm) _N	3.56	3.52	3.15	3.49	3.26	3.27
(Gd/Yb) _N	1.29	1.04	1.2	1.4	1.04	0.99
(La/Yb) _N	7.73	5.65	5.89	8.2	5.45	4.85
Eu/Eu*	0.59	0.61	0.61	0.51	0.63	0.61
Zr/Sc	58.11	32.59	21.71	61.97	26.37	40.45
Th/Sc	5.97	4.55	2.91	8.82	3.03	4.22
Th/Co	3.1	2.03	1.1	3.6	1.77	1.62
La/Th	0.96	0.71	0.87	0.90	0.90	0.61
La/Sc	5.76	3.23	2.55	8	2.73	2.6
Cr/Th	0.86	1.75	1.6	0.98	1.69	1.46

Table 1. (Continued.)

Sample no.	GCSL-7	GCSL-8	GCSL-9	GCSL-10	GCSL-11	GCSL-12	GCSL-13
Lat.	23°4'1.5''	23°4'1.7''	23°3'13.1''	23°3'14.1''	23°04'11.4''	23°03'27.1''	23°02'10.1''
Long.	73°39'51.5''	73°39'51.6''	73°40'20.9''	73°40'25.1''	73°40'34.7''	73°40'14.6''	73°38'53.2''
SiO ₂	57.94	51.85	62.96	60.09	51.37	52.89	51.43
Al ₂ O ₃	8.85	8.36	12.98	12.11	9.05	10.54	9.86
Fe ₂ O ₃	6.21	7.82	4.66	3.69	5.95	6.46	6.97
MnO	0.21	0.39	0.13	0.21	0.22	0.30	0.27
MgO	10.88	14.99	5.73	5.70	13.93	12.71	12.62
CaO	10.70	12.56	5.42	12.38	12.83	9.02	12.10
Na ₂ O	2.25	0.80	1.48	2.91	0.86	0.53	0.66
K ₂ O	0.53	1.58	3.39	0.39	2.48	3.11	1.94
TiO ₂	0.67	0.48	0.72	0.58	0.58	0.65	0.72
P ₂ O ₅	0.17	0.20	0.14	0.17	0.15	0.16	0.20
LOI	0.44	0.55	0.69	0.68	0.91	2.05	1.65
Sum	98.85	99.58	98.3	98.91	98.33	98.42	98.42
Sc	8.5	10.7	8.0	7.6	9.3	9.8	9.3
V	54	74	54	43	62	63	63
Cr	51	45	59	47	47	47	48
Co	20.3	24.1	17.1	10.6	22.7	21.5	22.3
Ni	25.2	28.4	27.4	24.9	27.8	28.8	27.9
Cu	11.8	10.2	12.9	11.2	10.9	29.3	11.6
Zn	86	85	57	69	73	88	79
Ga	42.5	45.2	46.2	33.1	39.6	45.8	44.4
Rb	241.5	499.1	1270.6	112.2	737.6	1547.7	637.3
Sr	154.5	142.0	155.3	200.2	122.2	90.1	124.9
Y	38.2	31.0	29.4	27.6	30.6	30.2	31.3
Zr	320.9	187.7	295.9	150.9	227.2	300.7	259.3
Nb	24.6	17.1	18.1	19.6	15.9	18.8	23.3
Cs	1.34	2.883	11.038	0.568	5.33	4.68	5.20
Ba	206	1218	2076	259	1533	1660	1445
La	38.6	26.3	32.0	28.1	29.0	27.1	19.7
Ce	79.0	53.7	65.5	60.0	59.8	61.0	40.6
Pr	8.6	6.0	6.9	6.6	6.5	5.8	4.4
Nd	34.9	24.1	27.3	25.7	26.1	23.2	17.8
Sm	7.3	5.1	5.7	5.5	5.5	4.9	3.9
Eu	1.3	0.9	1.0	1.0	1.0	0.9	0.7
Gd	5.9	4.3	4.6	4.5	4.5	4.2	3.6
Tb	1.0	0.7	0.8	0.8	0.8	0.8	0.7
Dy	6.6	5.2	5.2	5.0	5.2	5.4	5.0
Ho	1.4	1.1	1.1	1.0	1.1	1.2	1.1
Er	3.87	3.22	2.93	2.81	3.06	3.26	3.13
Tm	0.6	0.5	0.4	0.4	0.4	0.5	0.5
Yb	3.8	3.1	2.8	2.7	2.9	3.2	3.4
Lu	0.5	0.4	0.4	0.4	0.4	0.4	0.5
Hf	10.3	6.3	9.5	5.1	7.5	10.2	8.2
Ta	1.0	0.9	0.7	1.0	0.8	1.0	1.0
Pb	14.0	18.7	16.6	16.1	15.4	21.5	14.5
Th	38.2	26.2	37.2	31.6	31.2	39.1	36.4
U	2.0	0.9	1.9	0.9	1.6	1.2	1.5
(La/Sm) _N	3.37	3.27	3.62	3.25	3.38	3.52	3.21
(Gd/Yb) _N	1.27	1.13	1.34	1.37	1.28	1.06	0.88
(La/Yb) _N	7.16	5.93	9.15	7.3	7.08	5.94	4.11
Eu/Eu*	0.58	0.6	0.58	0.62	0.60	0.59	0.62
Zr/Sc	37.59	17.40	36.82	19.86	24.25	30.66	27.63
Th/Sc	4.47	2.43	4.63	4.15	3.33	3.99	3.88
Th/Co	1.87	1.08	2.17	2.95	1.37	1.81	1.63
La/Th	1.01	1	0.86	0.88	0.93	0.69	0.54
La/Sc	4.52	2.43	3.99	3.69	3.1	2.77	2.1
Cr/Th	1.34	1.72	1.58	1.51	1.50	1.21	1.33

$Eu/Eu^* = (Eu)_N / \sqrt{(Sm)_N * (Gd)_N}$.

distinguished by its high relief, weak pleochroism and two distinct sets of cleavages crossing almost at 90° angles. Actinolite can be seen nucleating along its margin, indicating its retrogression (figure 2d). Wedge or spindle shaped titanite grains with bold relief can be seen. Microcline is abundant (~30–40%), however, plagioclase (An₃₂–An₆₇) makes only 2–5% of the mode. Biotite commonly occurs along the margins of actinolite in the matrix of microcline. Its alteration to chlorite forms interdigitation, similarly, numerous pleochroic haloes are present in biotites. Epidote grains are anhedral, show higher order interference colours and commonly associated with actinolites. Subidioblastic scapolite grains can be seen in the form of granular clusters. They show prominent cleavages and moderate relief.

4. Bulk rock geochemistry

Thirteen representative samples of the calc-silicate rocks of the study area were analysed for determining major oxide, trace as well as rare earth elements (REEs) concentration. Major oxide data acquired using wavelength dispersive X-ray fluorescence (WD-XRF) using Philips MagiX PRO model PW 2440 wavelength dispersive X-ray fluorescence spectrometer coupled with automatic sample changer PW 2540, while trace elements and REEs have been analysed using high resolution inductively coupled plasma mass spectrometer (HR-ICP-MS; Nu Instruments Attom, UK) at the CSIR National Geophysical Research Institute, Hyderabad, following acid digestion that involves repeated treatment with HF–HNO₃–HClO₄. SARM-40 (South Africa) was used as standard.

Analytical results for major, trace and rare-earth elements are presented in table 1.

4.1 Major elements compositions

Analysed calc-silicate rocks exhibit a range of SiO₂ (51.4–64.9 wt.%) and Al₂O₃ (7.8–13.1 wt.%) which is lower than the average composition of post-archean upper continental crust (PAUCC), i.e., 65.9% and 15.17%, respectively, of Taylor and McLennan (1985), whereas MgO (5.7–15.6 wt.%), CaO (5.4–13.5 wt.%), FeO (3.7–6.9 wt.%), and MnO (0.1–0.4 wt.%) whole-rock compositions show enrichment relative to the compositions of PAUCC. The Harker plots show positive

correlation of SiO₂ with Al₂O₃, Na₂O, K₂O and TiO₂; whereas negative correlation with CaO, MgO, FeO, MnO, P₂O₅ and LOI (figure 3).

4.2 Trace elements compositions

Analysed calc-silicates show concentrations of Zn (61–91 ppm), Ga (27.6–50.2 ppm) and large-ion-lithophile elements (LILEs), viz., Rb (101.4–1547.7 ppm), Ba (156–2076 ppm) and Th (26.2–66.5 ppm) and high field strength elements (HFSEs), viz., Zr (150.9–467.8 ppm), Nb (15.9–29.8 ppm) Hf (5.1–15.0 ppm) which are higher compared to the PAUCC, whereas they are generally depleted in V (35–74 ppm), Cr (41–73 ppm), Ni (24.5–33.5 ppm), Cu (10.2–29.3 ppm) along with other LILEs, i.e., Sr (90.1–206.3 ppm) and U (0.9–3.0 ppm). Similarly, analyzed calc-silicates have concentrations of Co (10.6–24.4 ppm), another LILEs such as Cs (0.50–11.03 ppm), Pb (14.0–29.1 ppm) and another HFSE, viz., Ta (0.7–1.4 ppm) similar to PAUCC.

These rocks exhibit LREE-enriched but HREE-depleted subparallel chondrite-normalized REE patterns with moderately negative Eu anomalies (Eu/Eu*) ranging from 0.5 to 0.6 (figure 4). According to Taylor and McLennan (1985), negative Eu-anomaly indicates a typical continental crust composition and it is also a characteristic of post-archean sedimentary rocks, which is thus supplementing the fact, i.e., sedimentary protolith must be of post-archean age. As the plagioclase is a host mineral for Eu, its weathering and Eu-depleted source rocks may affect the intensity of negative Eu anomaly. These rocks reveal fractionated REE patterns (La_N/Yb_N = 4.1 to 9.1) with higher total REE abundances (up to 300 ppm).

REE patterns (including Eu anomalies) are influenced not only by provenance and sedimentary environment, but by climatic conditions also, present at the time of deposition of rocks (Yanjing and Yongchao 1997). Based on the studies of the early Precambrian sediments from the North China craton, these workers have convincingly argued that the high total REE and Eu depletion are the characteristics of the sediments deposited in oxidizing conditions (i.e., fO₂ is high), similarly, reverse being true. Banded iron formations, red beds, etc. found to be residing within the Proterozoic rocks from all over the world also supports this concept.

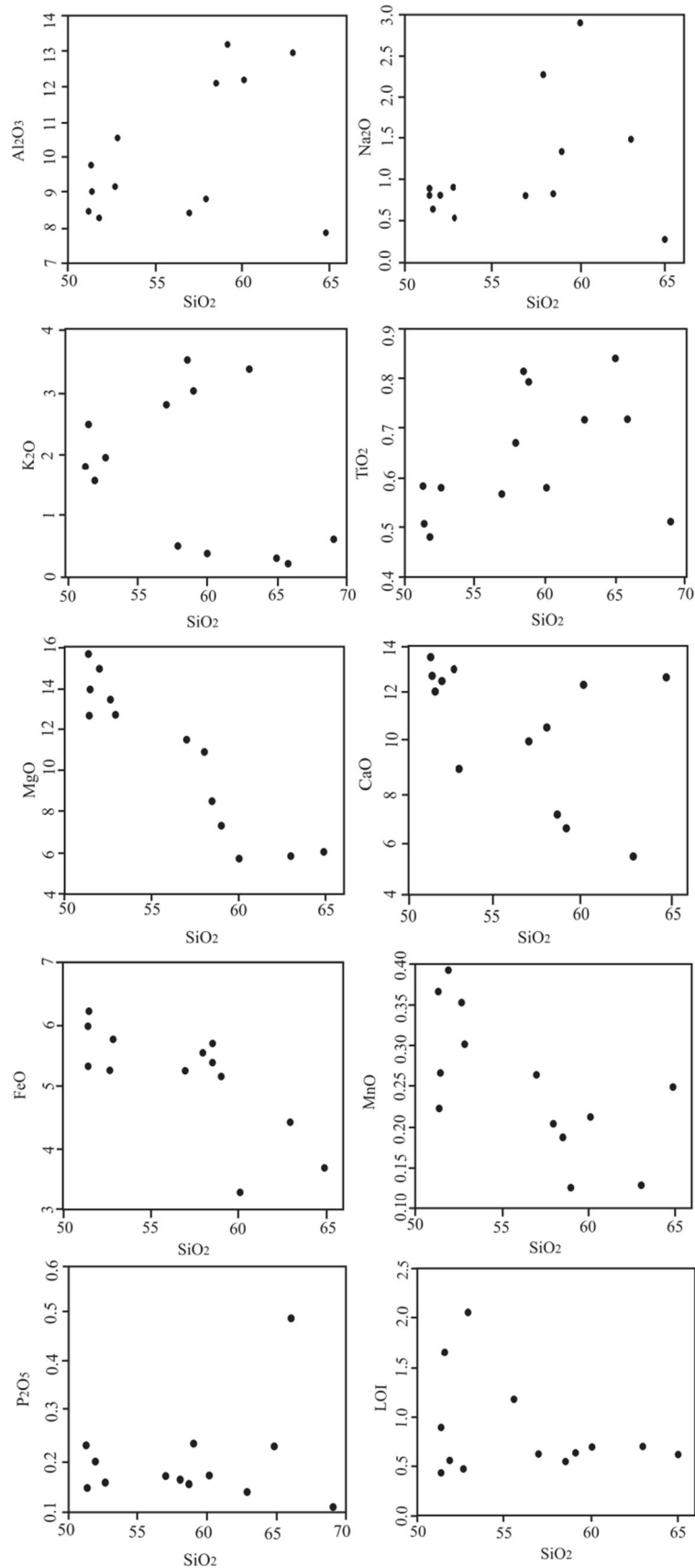


Figure 3. Whole-rock concentrations of major-element *vs.* silica in weight percent oxides for calc-silicates samples of Lunavada. Concentrations of all major elements excluding Al₂O₃, K₂O, Na₂O and TiO₂ exhibit near-linear inverse correlations with SiO₂. *All irons are reported as FeO.

5. Discussion

5.1 Protolith of calc-silicate rocks

Certain metamorphic events and other alterations may have significantly affected mobility of some elements such as Si, Na, K, Ca, Mg, Rb, and Sr of parent material of these calc-silicates which are embedded within the metapelites present in the study area. Hence relatively immobile elements such as the HREEs, HFSEs, Cr, Co, Th and Sc can be considered most reliable for protolith determination (Taylor and McLennan 1985; Bhatia and Crook 1986). They are insensitive to the igneous and sedimentary fractionation processes (Garcia *et al.* 1991; McLennan *et al.* 1993; Garcia *et al.* 1994; Polat and Hofmann 2003) and generally pass on to the sediments quite unfractionated during sedimentary processes thus leaving the signatures of parent material within those sediments (Nance and Taylor 1977; Taylor and McLennan 1985; McDaniel *et al.* 1994).

Relative proportions of major-elements such as SiO₂, CaO, Al₂O₃, FeO, and MgO reveal whether the calc-silicates possess a carbonate/silicate-rich clastic protoliths or metasomatic origins (Barton *et al.* 1991; Tracy and Frost 1991). Calc-silicate bulk-rock compositions normalized to CaO, Al₂O₃, and FeO + MgO correspond closely to the compositions of marls and calcareous sandstone (Petrijohn 1984). On CaO, Al₂O₃ and FeO + MgO ternary diagram, most of the calc-silicate samples fall within or very near to greywacke zone (figure 5). Hence, the near-linear negative correlation of CaO, MgO, FeO, MnO, P₂O₅ and LOI with SiO₂ observed within sample areas may therefore be due to quartz dilution related to variable amounts of quartzo-feldspathic material and clay within protolith.

The positive correlation between Al₂O₃ and nearly all measured trace elements implies that these elements are primarily controlled by the K-bearing minerals, i.e., clay minerals and micas. Similarly, positive correlation of Al₂O₃ with Na₂O and K₂O indicates that the K-bearing minerals exert significant control over the Al distribution (figure 6), thus further suggesting that the protolith must have been bound to clay (McLennan *et al.* 1990; Condie *et al.* 2001).

Enrichment of heavy mineral zircon in these calc-silicates is often due to its accumulation with quartz in the sand fraction during sedimentation and recycling (Taylor and McLennan 1985;

McLennan 1989; McLennan *et al.* 1990). Similarly, enrichments of Ba in silica-rich samples are also seen which indicate that Zr and Ba are positively correlated with SiO₂. Ba is also having positive correlation with K₂O may reflect a celsian component in detrital potassium-feldspars and deposited with quartz in the sandy portion of the protolith, as potassium-feldspar is more resistant to chemical weathering than plagioclase (Nesbitt and Young 1989). In these rocks, abundant microcline is present. This fact supports the hypothesis of accumulation of potash feldspar in fluvial sands on account of source which must be mostly granitic (Nesbitt *et al.* 1996).

In the study area, the quartzite-metapelite sequence suggests the transition from sandstone to shale which denotes the sedimentary facies transitions from shallow-water shelf deposits to deep-water slope deposits. As the calc-silicate samples fall closer to sandstone zone on the Al–Zr–Ti diagram (figure 7) of Garcia *et al.* (1994) which shows a sandstone-shale continuum, shallow-water shelf depositional environment is indicated for primary sediments. Near linear variation of sample plots on this sandstone-shale continuum reflects the bimodal character of these rocks due to alternating cycles of sandstones and shale deposition, across strike within the study area which again supports the protolith having mixture and varying proportions of quartzo-feldspathic material and clay.

5.2 Source area weathering

Weathering of the source rocks is affected by factors such as properties and mineral composition of the parent rocks and the climate. According to Sawyer (1986) and Nesbitt *et al.* (1996), weathering in source area ultimately affects the composition of clastic sedimentary rocks or the protolith of any metamorphic rock.

Nesbitt and Young (1982) proposed the Chemical Index of Alteration (CIA) as a measure of the degree of chemical weathering/alteration of the source rocks. They have put forward the calculation where CIA is equal to $[Al_2O_3/(Al_2O_3 + CaO^* + Na_2O + K_2O)] * 100$. The values of oxides are in molecular proportions and CaO* represents CaO in silicate minerals only. The CIA values for calc-silicate rocks were calculated and plotted in the conventional Al₂O₃–(CaO+Na₂O)–K₂O (A–CN–K) ternary diagram (figure 8). It has been

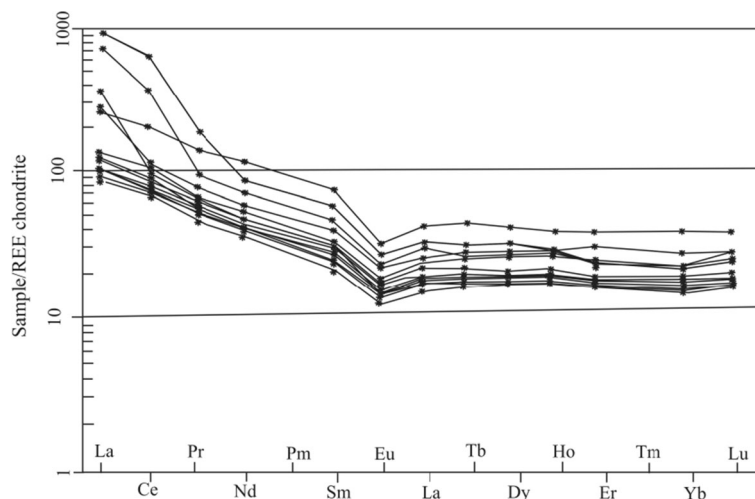


Figure 4. Chondrite normalized rare earth elements (REEs) patterns for calc-silicates of the study area (after Sun and McDonough 1989).

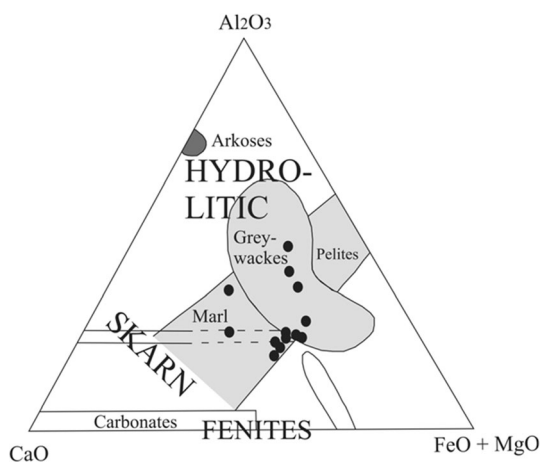


Figure 5. The bulk-rock compositions of calc-silicates are plotted on a CaO–Al₂O₃–FeO+MgO (wt.%) ternary diagram. General bulk compositions of unaltered arkoses, pelites, greywackes and marls are represented by shaded fields along with schematic regions for metamorphic types (after Barton *et al.* 1991).

observed that the calculated CIA values for calc-silicate rocks are low to moderate, i.e., 50–86 with average = 63 which indicates low to moderate weathering. Most of the samples plot in the upper part of the diagram having inclination towards the illite composition, thus indicating moderate degree of alteration.

Low CIA values indicate near absence of chemical alteration which may reflect cold and/or arid conditions or alternatively rapid physical weathering (Singh and Khan 2017) probably in a subtropical condition. Thus cold and arid climatic conditions must have had a control over the weathering of source rocks for the calc-silicates under study. Major elements such as Ca, Na and K

are highly mobile and likely to get affected by weathering processes (Nesbitt *et al.* 1980; Nesbitt and Young 1982), but Al₂O₃ remains as a residual product as it is immobile relatively.

5.3 Provenance

Immobile elements like Zr, Ti, Y, Nb, Cr, Sc, La, Th, Ce and Nd are often used to infer the paleotectonic environments of metamorphic rocks (Nutman *et al.* 2010; Giere *et al.* 2011), apart from their role in protolith determination. Th/Sc ratio is directly proportional to Zr/Sc ratio during igneous differentiation, but as zircon enrichment in sediments affects this relation, Th/Sc *vs.* Zr/Sc diagram (McLennan *et al.* 1993) also serves as a good indicator to assess the sediment recycling (Ahmad *et al.* 2016). The Th/Sc–Zr/Sc plot (figure 9) can distinguish between evolved and juvenile sediment sources and the extent of sorting and recycling experienced by sediments (Taylor and McLennan 1985; McLennan *et al.* 1990), thus distinguishing the effects of source composition and sedimentary process on the basis of assumption that quartz dilution would result in preferential enrichment in Zr and to some extent, in Th (McLennan and Taylor 1991). This is based on the general trend of higher Th/Sc (≥ 1) and Zr/Sc (≥ 10) values in sediments derived from evolved continental sediment sources relative to sediments supplied by juvenile, mafic sources (Roser *et al.* 1996). Detritus from felsic rocks of the UCC have an average ratio equal to or greater than 0.79, while values less than 0.6 suggest mafic and ultramafic components (McLennan *et al.* 1990).

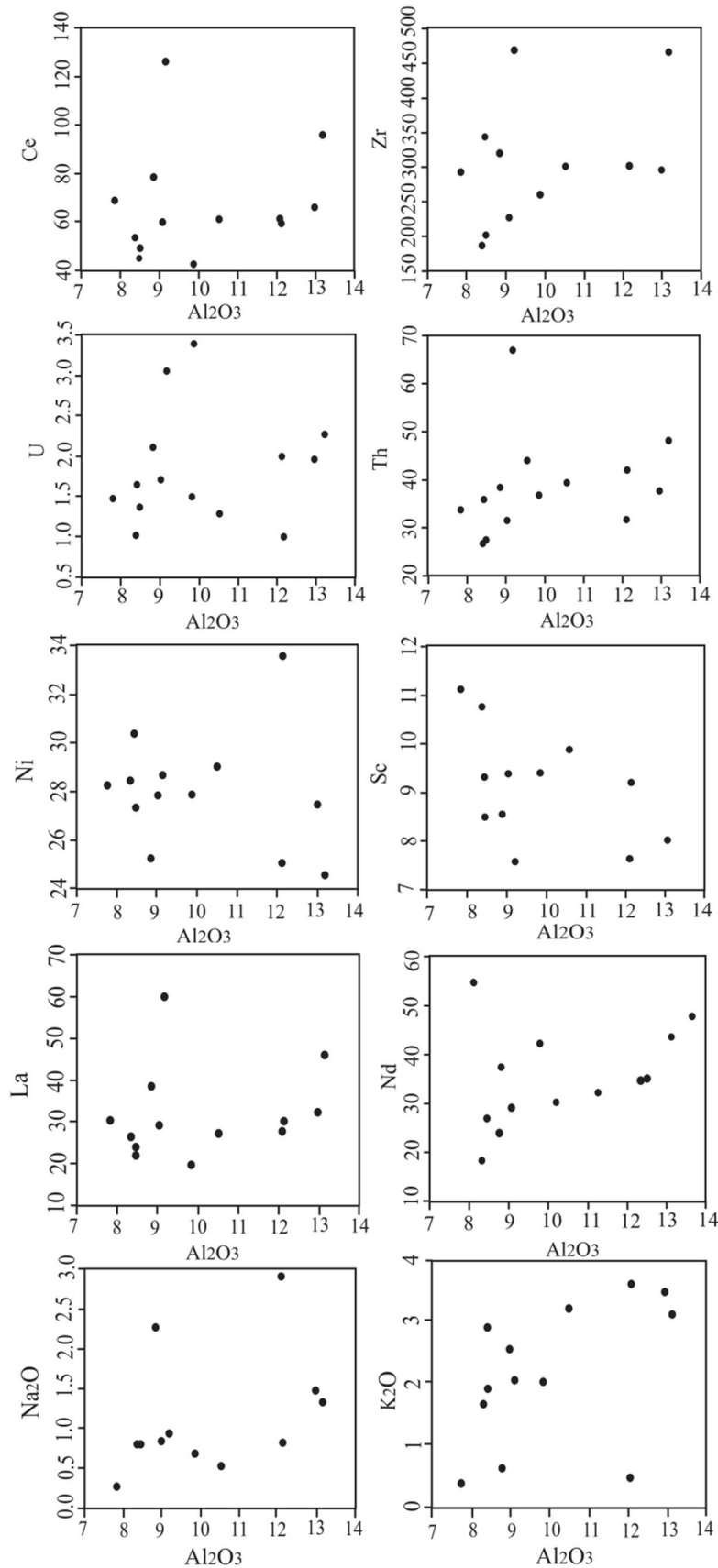


Figure 6. Whole-rock compositions of selected trace-elements along with Na₂O and K₂O exhibit a positive correlation with Al₂O₃ in these calc-silicates (with the exception of Ni and Sc) suggesting these components were bound in clays.

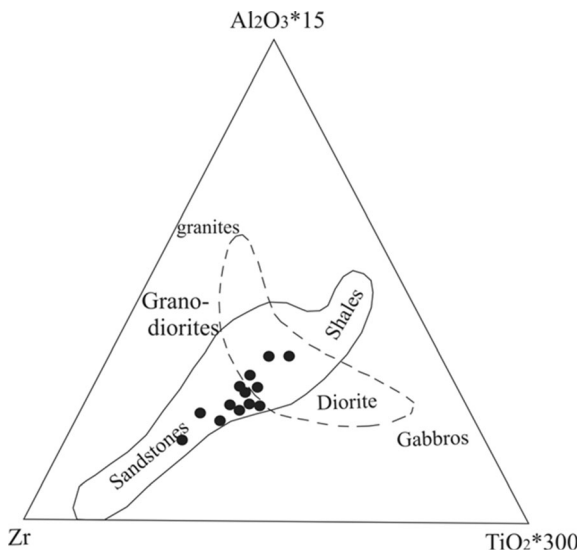


Figure 7. Whole-rock compositions of calc-silicates fall within the continuum between sandstone and shale (grey) on a ternary Al–Zr–Ti diagram (after Garcia *et al.* 1994). The field outlined by the dashed line represents the typical curved trend exhibited in whole-rock compositions of rocks derived from calc-alkaline plutonic suites.

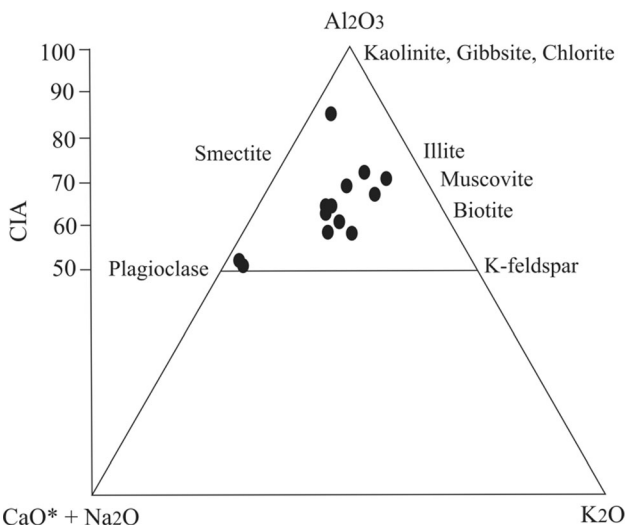


Figure 8. A–CN–K diagram (after Nesbitt and Young 1982) using molar proportions of Al_2O_3 , CaO , Na_2O and K_2O . As per the CIA scale, sample plots of calc-silicates indicate low to moderate weathering of source rocks.

Th/Sc ratio of greater than 0.79 is shown by these calc-silicate rocks thus suggesting a provenance from a felsic source. Similarly, detritus derived from a felsic source tend to be enriched in incompatible elements like Th, Zr and La, whereas those derived from a mafic source are enriched in compatible elements like Sc, Cr and Co (Ahmad *et al.* 2016). Here, it has been observed that the calc-silicate rocks of the study area show enrichment in the incompatible elements, viz., Th, Zr and La and are depleted in Sc,

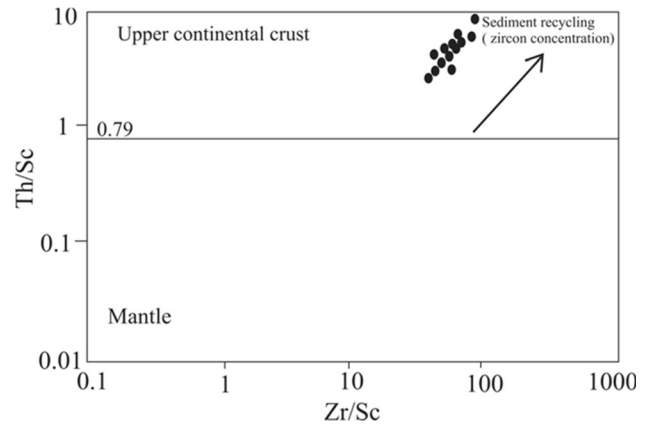


Figure 9. Th/Sc vs. Zr/Sc ratio diagram showing the composition of the sources for the primary sediments of calc-silicate rocks and the extent of recycling or concentration of Zr in sediments, associated with the abundance of heavy minerals, particularly zircon (after McLennan *et al.* 1990).

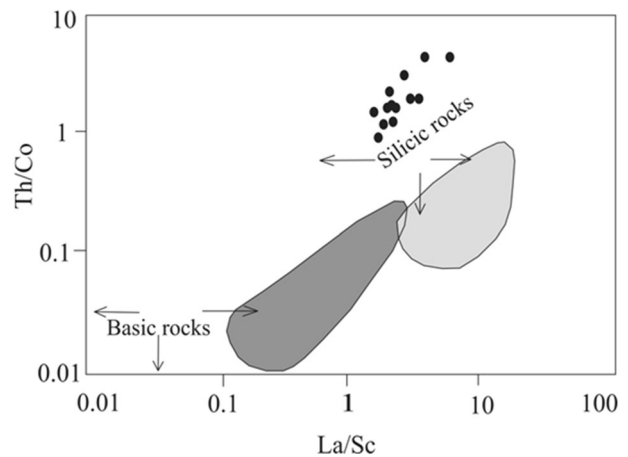


Figure 10. Th/Co vs. La/Sc diagram (after Cullers 2002) where sample data plotted can be seen to be showing affinity towards the source rocks of homogeneous composition of felsic nature.

Cr and Co, thus emphasizing the felsic nature of provenance. Apart from Th/Sc, other elemental ratios between immobile elements such as La/Sc, Th/Co, and Cr/Th are the robust indicators of provenance (Wronkiewicz and Condie 1990; Cullers 1994). Th/Sc (2.4–8.8), La/Sc (2.1–8), Th/Co (1.1–3.6) and Cr/Th (0.8–1.7) ratios also support the sediment derivation from mostly homogeneous sources with major contribution from the felsic component. Calc-silicate samples fall in an array indicative of felsic composition of the source rocks in Th/Co vs. La/Sc bivariate plot, i.e., figure 10 (Cullers 2002). Trace element studies revealed that the source of these calc-silicates was similar in composition to the average post-archean upper continental crust, mostly granitic thus supporting

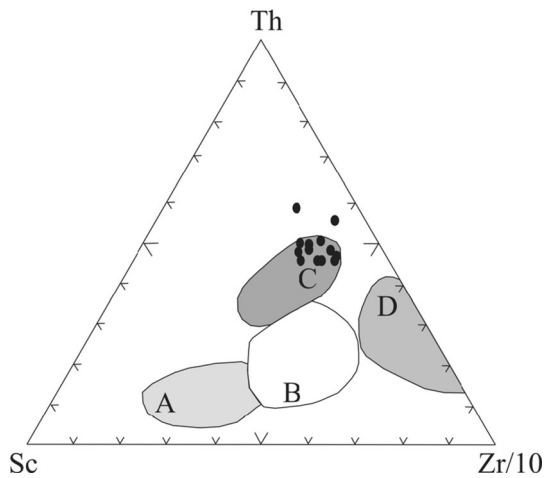


Figure 11. Sc–Th–Zr/10 diagram of Bhatia and Crook (1986), A: oceanic island arc; B: continental island arc; C: active continental margin; D: passive/rifted margins; calc-silicate samples fall in the ‘C’ region of this diagram indicating deposition of primary sediments in active continental margin setting.

an idea that a significant amount of differentiated felsic igneous rocks probably present in the source area at the onset of sedimentation.

5.4 Tectonic setting

The tectonic settings in which sedimentary rocks are deposited also exert a control over the geochemistry of those rocks to large extent (Bhatia and Crook 1986; Roser and Korsch 1986; McLennan *et al.* 1990).

The immobile trace elements (as mentioned earlier) are also used to determine the paleo-tectonic setting of clastic sediments (Bhatia and Crook 1986; McLennan *et al.* 1990). Here, Sc–Th–Zr/10 plot of Bhatia and Crook (1986) has been used because it can discriminate the sediments from passive margin to active continental margin settings. It can be seen that the sample data are plotted within the field of active continental margin on this diagram (e.g., Sc=8.49 ppm, Th=35.92 ppm, Zr=343.69 ppm; figure 11). Deposited sediments at the active continental margin are poorly sorted, less recycled as well as are having less maturity than those deposited at the passive continental margin (Roser *et al.* 1996).

6. Conclusion

The calc-silicate rocks show major oxides, trace and rare earth element compositions that closely resemble to those of their post-archean

counterparts suggesting that the chemical composition of continental crust of the study area was similar to that of post-Archean crust which is also supported by the REEs *vs.* sample/REE chondrite normalized pattern in which moderate negative Eu anomaly is suggestive of post-archean continental crust. On the basis of Al₂O₃, CaO and FeO+MgO diagram of Barton *et al.* (1991) where most of the samples fall within or very close to greywacke zone, it can be concluded that the protolith of calc-silicate rocks of the study area must be calcareous sandstone with small and varied amounts of clay within it. CIA studies are pointing towards the low to moderate weathering of source under cold and arid conditions. The Th–Sc characteristics (Th/Sc > 1) support a predominantly continental source for these rocks, similarly values of Zr/Sc indicate moderate amount of sediment recycling. Higher abundances of incompatible elements imply predominantly felsic rocks in the source, further approved by LREE enriched patterns. Also, as per the Th/Co *vs.* La/Sc plot, a predominantly felsic source, i.e., mostly of granitic composition is inferred for primary sediments for these calc-silicate rocks. Lastly, it is concluded that the primary sediments for the calc-silicates of the Lunavada Group were deposited in an active continental margin setting.

Acknowledgements

The authors are thankful to Prof. H Kataria, Dean, Faculty of Science and I/c Head, Department of Geology, MSUB, for extending facilities and granting permission to carry out this research. The authors are grateful to the Director of the CSIR-NGRI, Hyderabad for extending the analytical facilities. Dr. K S V Subramanyam, Dr. D Purushotham, Dr. M Ram Mohan and Dr. M Satyanarayanan of the CSIR-NGRI are sincerely thanked for the help rendered during sample preparation and analysis. The first author is also thankful to the DST-Women Scientist (WOS-A) project, for providing funding to carry out this work. We also thank Editor-in-Chief, Prof. N V Chalapathi Rao and Prof. Rajneesh Bhutani (Handling Editor), for smooth handling of the MS. We are indebted to two anonymous reviewers for their constructive comments and suggestions which improved the manuscript considerably.

Author Statement

Gayatri Akolkar: Conceptualization, methodology, funding acquisition, sample analysis, data curation, data interpretation and writing base draft. M A Limaye: Supervision of the project, data interpretation, and presentation.

References

- Ahmad I, Mondal M E A and Satyanarayanan M 2016 Geochemistry of Archean metasedimentary rocks of the Aravalli craton, NW India: Implications for provenance, paleoweathering and supercontinent reconstruction; *J. Asian Earth Sci.* **126** 58–73.
- Akolkar G, Joshi A U, Limaye M A and Deota B S 2018 Implication of Godhra granite emplacement on calc-silicate rocks of Lunavada Region, NE Gujarat; *J. Geosci. Res.* **3** 147–152.
- Barton M D, Ilchik R P and Marikos M A 1991 Metasomatism; *Rev. Mineral.* **26** 321–350.
- Bhaskar Rao B 1986 *Metamorphic Petrology*; CRC Press, Boca Raton, 182p.
- Bhatia M R and Crook K A W 1986 Trace elements characteristics of greywacke and tectonic setting discrimination of sedimentary basins; *Contrib. Mineral. Petrol.* **92** 181–193.
- Condie K C, Lee D and Farmer G L 2001 Tectonic setting and provenance of the Neoproterozoic Uinta Mountain and Big Cottonwood groups, northern Utah: Constraints from geochemistry, Nd isotopes, and detrital modes; *Sedim. Geol.* **141** 443–464.
- Cullers R L 1994 The controls on the major and trace element variation of shales, siltstones, and sandstones of Pennsylvanian–Permian age from uplifted continental blocks in Colorado to platform sediment in Kansas, USA; *Geochim. Cosmochim. Acta* **58** 4955–4972.
- Cullers R L 2002 Implications of elemental concentrations for provenance, redox conditions, and metamorphic studies of shales and limestones near Pueblo, CO, USA; *Chem. Geol.* **191** 305–327.
- Garcia D, Coelho J and Perrin M 1991 Fractionation between TiO₂ and Zr as a Measure of Sorting within Shale and Sandstone Series (Northern Portugal); *Eur. J. Mineral.* **3** 401–414.
- Garcia D, Fontelles M and Moutte J 1994 Sedimentary fractionations between Al, Ti, and Zr and the genesis of strongly peraluminous granites; *J. Geol.* **102** 411–422.
- Giere R, Rumble D, Gunther D, Connolly J and Caddick M J 2011 Correlation of growth and breakdown of major and accessory minerals in metapelites from Campolungo, Central Alps; *J. Petrol.* **52** 2293–2334.
- Gopalan K, Trivedi J R, Merh S S, Patel P P and Patel S G 1979 Rb–Sr age of Godhra and related granites, Gujarat (India); *Proc. Indian Acad. Sci. (Earth Planet. Sci.)* **88A** 7–17.
- Gupta B C and Mukherjee P N 1938 Geology of Gujarat and Southern Rajputana; *Rec. Geol. Surv. India* **73** 163–208.
- Gupta S N, Arora Y K, Mathur R K, Iqbaluddin B P, Sahai T N and Sharma S B 1995 Geological map of the Precambrians of the Aravalli Region, Southern Rajasthan and northeastern Gujarat, India; *Geol. Surv. India Publ.*, Hyderabad.
- Gupta S N, Arora Y K, Mathur R K, Iqbaluddin B P, Sahai T N and Sharma S B 1980 Lithostratigraphic map of Aravalli Region, southern Rajasthan and northeastern Gujarat; *Geol. Surv. Ind. Publ.*, Hyderabad.
- Gupta S N, Arora Y K, Mathur R K, Iqbaluddin B P, Sahai T N and Sharma S B 1997 The Precambrian geology of the Aravalli region, southern Rajasthan and northeastern Gujarat; *Geol. Surv. India Memoir* **123** 58–65.
- Gupta S N, Mathur R K and Arora Y K 1992 Lithostratigraphy of Proterozoic rocks of Rajasthan and Gujarat; *Rec. Geol. Surv. India, A Rev.* **115** 63–85.
- Iqbaluddin and Venkataramaiah T 1976 Photogeological mapping with selective checks in parts of Kadana Reservoir area, Panchmahal district, Gujarat; Rep. (Unpublished) *Geol. Surv. India (F.S.1975–76)*.
- Iqbaluddin B P 1989 Geology of Kadana Reservoir Area, Panchmahals District, Gujarat and Banswara and Durgapur districts, Rajasthan; *Geol. Surv. India Memoir* **121** 84.
- Joshi A U, Limaye M A and Deota B S 2016 Microstructural indicators of post-deformational brittle-ductile shear zones, Lunawada region, Southern Aravalli Mountain Belt, Gujarat, India; *JMSUST* **51(1)** 19–27.
- Mamtani M A 1998 Deformational mechanisms of the Lunavada Pre-Cambrian rocks, Panchmahal district, Gujarat; Unpublished PhD thesis, The M.S. University of Baroda, India.
- Mamtani M A and Greiling R O 2005 Granite emplacement and its relation with regional deformation in the Aravalli Mountain Belt (India) – inferences from magnetic fabric; *J. Struct. Geol.* **27** 2008–2029.
- Mamtani M A, Greiling R O, Karanth R V and Merh S S 1999 Orogenic deformation and its relation with AMS fabric – an example from the Southern Aravalli Mountain Belt, India; In: The Indian subcontinent and Gondwana: A Palaeomagnetic and rock magnetic perspective (eds) Radhakrishna T and Piper J D, *Geol. Soc. India Memoir* **44** 9–24.
- Mamtani M A, Karanth R V, Merh S S and Greiling R O 2000 Tectonic evolution of the Southern part of Aravalli Mountain Belt and its environs – possible causes and time constraints; *Gondwana Res.* **3** 175–187.
- Mamtani M A, Karmakar I B and Merh S S 2002 Evidence of polyphase deformation in gneissic rocks around Devgadhi Bariya: Implications for evolution of Godhra Granite in the Southern Aravalli Region (India); *Gondwana Res.* **5(2)** 401–408.
- Mamtani M A, Merh S S, Karanth R V and Greiling R O 2001 Time relationship between metamorphism and deformation in the Proterozoic rocks of Lunavada region, southern Aravalli Mountain Belt (India) – a microstructural study; *J. Asian Earth Sci.* **19** 195–205.
- McDaniel D K, Hemming S R, McLennan S M and Hanson G N 1994 Resetting of neodymium isotopes and redistribution of REEs during sedimentary processes: The early Proterozoic Chelmsford Formation, Sudbury Basin, Ontario, Canada; *Geochim. Cosmochim. Acta* **58** 931–941.
- McLennan S M 1989 Rare earth elements in sedimentary rocks: Influence of provenance and sedimentary processes; Mineralogical Society of America; *Rev. Mineral.* **21** 169–200.

- McLennan S M and Taylor S R 1991 Sedimentary rocks and crustal evolution: Tectonic setting and secular trends; *J. Geol.* **99** 1–21.
- McLennan S M, Hemming S, McDaniel D K and Hanson G N 1993 Geochemical approaches to sedimentation, provenance, and tectonics; *Geol. Soc. Am. Spec. Paper* **284** 21–40.
- McLennan S M, Taylor S R, McCulloch M T and Maynard J B 1990 Geochemical and Nd–Sr isotopic composition of deep-sea turbidites – crustal evolution and plate tectonic associations; *Geochim. Cosmochim. Acta* **54** 2015–2050.
- Merh S S 1995 *Geology of Gujarat*; Geological Society of India, Bangalore.
- Nance W B and Taylor S R 1977 Rare earth element patterns and crustal evolution. II: Archean sedimentary rocks from Kalgoorlie, Australia; *Geochim. Cosmochim. Acta* **41** 225–231.
- Nesbitt H W and Young G M 1982 Early Proterozoic climates and plate motions inferred from major element chemistry of lutites; *Nature* **299** 715–717.
- Nesbitt H W and Young G M 1989 Formation and diagenesis of weathering profile; *J. Geol.* **97** 129–147.
- Nesbitt H W, Markovics G and Price R C 1980 Chemical processes affecting alkalis and alkaline earths during continental weathering; *Geochim. Cosmochim. Acta* **44** 1659–1666.
- Nesbitt H W, McLennan S M and Keays R R 1996 Effects of chemical weathering and sorting on the petrogenesis of siliciclastic sediments, with implications for provenance studies; *J. Geol.* **104** 525–542.
- Nutman A P, Friend C R L, Bennett V C, Wright D and Norman M D 2010 \geq 3700 Ma pre-metamorphic dolomite formed by microbial mediation in the Isua supracrustal belt (W Greenland): Simple evidence for early life?; *Precamb. Res.* **183** 725–737.
- Pettijohn F J 1984 *Sedimentary Rocks*; CBS Publishers, New Delhi.
- Polat A and Hofmann A W 2003 Alteration and geochemical patterns in the 3.7–3.8 Ga Isua greenstone belt, West Greenland; *Precamb. Res.* **126** 197–218.
- Roser B P and Korsch R J 1986 Determination of tectonic setting of sandstone-mudstone suites using SiO₂ content and K₂O/Na₂O ratio; *J. Geol.* **94** 635–650.
- Roser B P, Cooper R A, Nathan S and Tulloch A J 1996 Reconnaissance sandstone geochemistry, provenance and tectonic setting of the lower Paleozoic terranes of the West Coast and Nelson, New Zealand; *New Zeal. J. Geol. Geophys.* **39** 1–16.
- Sawyer E W 1986 The influence of source rock type, chemical weathering and sorting on the geochemistry of clastic sediments from the Quebec metasedimentary belt, Superior Province, Canada; *Chem. Geol.* **55** 77–93.
- Sen K and Mamtani M A 2006 Magnetic fabric, shape preferred orientation and regional strain in granitic rocks; *J. Struct. Geol.* **28** 1870–1882.
- Singh P K and Khan M S 2017 Geochemistry of Palaeoproterozoic rocks of Aravalli supergroup: Implications for weathering history and depositional sequence; *Int. J. Geosci.* **8** 1278–1299.
- Sun S and McDonough W F 1989 Chemical and isotopic systematics of oceanic basalts: Implications for mantle composition and processes; *Geol. Soc. Lond., Spec. Publ.* **42** 313–345.
- Taylor S R and McLennan S M 1985 *The Continental Crust: Its Composition and Evolution*, Blackwell Scientific Publications, Oxford.
- Tracy R J and Frost B R 1991 Phase-equilibria and thermobarometry of calcareous, ultramafic and mafic rocks, and iron formations; *Rev. Mineral.* **26** 207–289.
- Wronkiewicz D J and Condie K C 1990 Geochemistry and mineralogy of sediments from the Ventersdorp and Transvaal Supergroups, South Africa: Cratonic evolution during the early Proterozoic; *Geochim. Cosmochim. Acta* **54** 343–354.
- Yanjing C and Yongchao Z 1997 Geochemical characteristics and evolution of REE in the early Precambrian sediments: Evidence from the southern margin of the North China craton; *Episodes* **20** 109–116.



Implication of Godhra Granite Emplacement on Calc-silicate Rocks of Lunavada Region, NE Gujarat

Gayatri Akolkar, Aditya U. Joshi, M. A. Limaye* and Bhushan S. Deota

Department of Geology, Faculty of Science, M.S. University of Baroda, Vadodara-390002, India

*E-mail: manoj_geol@rediffmail.com

Abstract

The Lunavada region of NE Gujarat is characterised by discontinuous lensoidal bodies of calc-silicate rocks belonging to the Kadana Formation of Lunavada Group, upper Aravallis. These calc-silicates bands are sandwiched between quartzite-metapelite intercalations that occur at lower elevations. Various mineral assemblages within calc-silicates has two petrographic distinctions. Type-1 calc-silicates with un-oriented actinolite needles consists minerals in order of their decreasing abundance as Act + Di + Cal + Qtz + Sph ± Mc ± Pl ± Bt ± Ep ± Chl. Type-2 calc-silicates contain un-oriented hornblende laths with skeletal almandine garnets having dominant mineral assemblage of Hbl + Grt + Qtz + Pl + Cal + Mus + Chl + Sph + Ep. Both the types subsists minor proportion of zircon and opaques. Established time relationship of metamorphic crystallisation with deformation on meta-pelites of Lunavada region signifies no syn-post emplacement growth, while minerals like actinolite/hornblende and garnet within calc-silicates show overprinting and exhibit signatures of syn-to-late stage of metamorphic crystallisation.

Keywords: Lunavada, Kadana, Calc-silicate, Metamorphic crystallisation, Microstructures

Introduction

The Lunavada region situated at NE Gujarat comprises exposures of the Lunavada Group, a part of Southern Aravalli Mountain Belt (SAMB) in Gujarat (Fig.1). These rocks are of Meso-Proterozoic age and represent the youngest formation of Lunavada Group within the Aravalli Supergroup (Iqbaluddin, 1989; Gupta *et al.*, 1992; 1997) (Table 1). Rocks of this region exhibit an intercalated sequence of quartzite-metapelite with minor occurrences of calc-silicate rock as discontinuous bands and lenses (Mamtani, 1998; Mamtani *et al.*, 2000). Godhra granite as a significant pluton obscures its southern and south-western boundary, whereas the western margin shows overlapping of younger extrusive basaltic rocks (Gupta *et al.*, 1980; 1995). The Lunavada terrain is also well known for its regional scale tectonics and analogous micro-scale derivatives (Mamtani *et al.*, 2001). The present work signifies first hand microscopic evidences of these calc-silicates in terms of its petrographic distinction and highlights generation of minerals in response to the neighbouring pluton. With the help of existing mineral growth records through microstructural analysis, the present work claims inherent refinement by proposing the effect of thermal metamorphism on the calc-

silicate rocks during syn-post phases of granite emplacement.

Geological and Structural Setting

Lunavada Group of rocks exposed in NE Gujarat are identified as a part of SAMB and assigned the status of second youngest group in the Aravalli Supergroup. These rocks mark the polygonal shaped outline, which occupies an area of >10,000km². Chief rock-types of the Lunavada Group are meta-pelites, quartzites, meta-subgreywackes, petromict meta-conglomerates with minor layers of marble and phosphatic algal meta-dolomites (Gupta *et al.*, 1980, 1992, 1995, 1997). The said lithological sequences are invaded by Neo-Proterozoic Godhra intrusives of 955±20Ma (Gopalan *et al.*, 1979). The grade of regional metamorphism has reached up to lower amphibolite facies condition by the development of chlorite grade in the northern part to garnet grade in the southern part within the schistose rocks of the Lunavada terrain (Mamtani, 1998; Mamtani *et al.*, 2001). Structurally, rocks of the Lunavada region are affected by three deformational episodes. D₁ and D₂ are coaxial with NE-SW striking axial traces, where as D₃ marks the NW-SE trend and is coeval with the granite emplacement (Mamtani *et al.*, 2001;

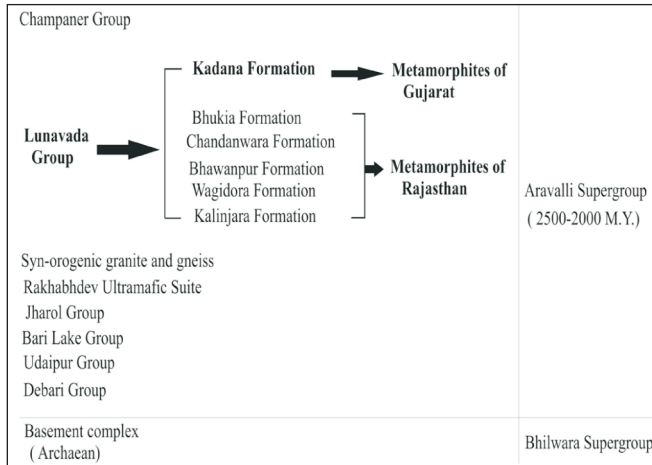


Table 1: Proterozoic succession of North Gujarat and South Rajasthan (modified after Gupta *et al.*, 1980; 1992).

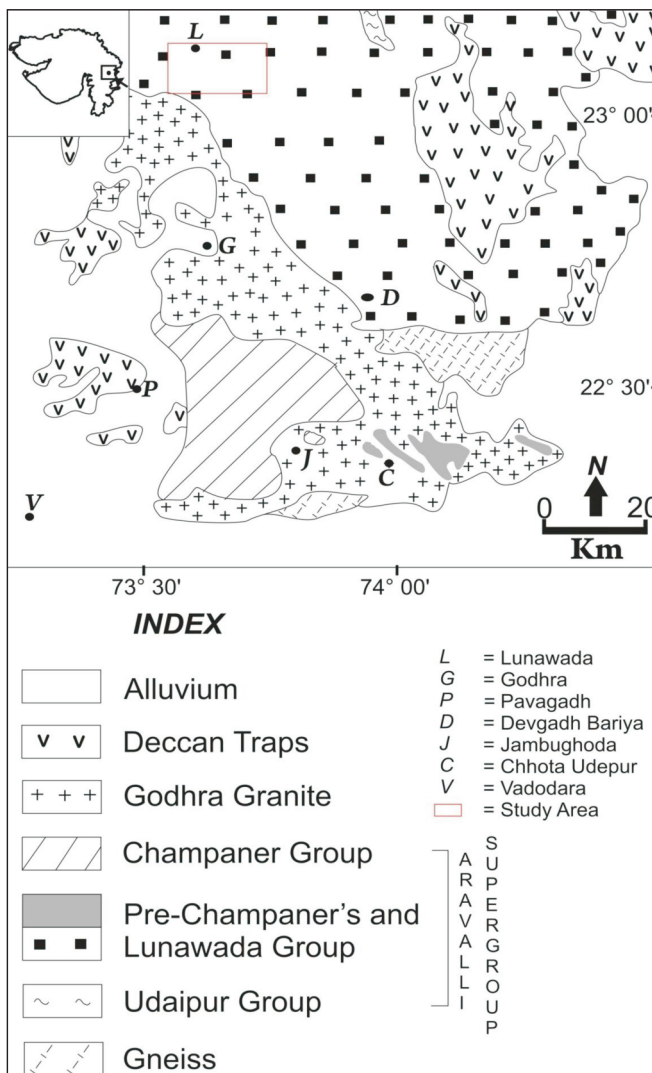


Fig.1. Lithostratigraphic map of Southern Aravalli mountain belt (SAMB) (modified after Mamtani *et al.*, 2005).

Mamtani and Greiling, 2005; Mamtani *et al.*, 2002; Sen and Mamtani, 2006). Several NW-SE trending axial planar slippages have also been recorded with the last phase of deformation (Mamtani *et al.*, 1999; Joshi *et al.*, 2016). The area selected for the study lie SE of Lunavada town, which comprises intercalated sequence of quartzite-metapelite with minor bands and lenses of calc-silicate rocks (Fig. 2). These rocks belong to the Kadana Formation of the Lunavada Group, Aravalli Supergroup.

Field exposures of the Type-1 calc-silicate rocks located at the southern part of the study area nearer to granite display well defined maculose structure (Fig 3a). The thick band of Type-1 calc-silicates resides within the core of D₁ and D₂ fold. The rock is massive in nature and exhibit dark grey appearance. Protruding porphyroblasts of un-oriented actinolites are well developed over the upper and inner surfaces. The calc-silicate rocks in contact with the adjacent quartzite-metapelite intercalations show marginal orientation of these needles. The average length of needles present within the southern part ranges from 0.5 to 1 cm. At places, the present variety is enriched in quartz vein of folded nature embedded in these calc-silicate rocks (Fig. 3b). However, few associations with granite-pegmatites of discordant nature were encountered along the southern most margins (Fig. 3c). Type-2 calc-silicate variety is mainly restricted to the northern part of the study area. The present variety consists of thin band as compared to the former. The rock exhibit dirty white appearance with the development of tiny dark green un-oriented hornblende needles of 0.2 to 0.5 cm in length (Fig 3d). Both the types prominently exhibit regional foliation striking NE-SW with 47° of north-westerly dip.

Petrography

Petrographic analysis of calc-silicate rocks exhibit hornfelsic texture as a major texture with poikiloblastic texture as a minor texture (Fig. 4a). There exists variation in terms of mineral assemblages in both the types of calc-silicate rocks. Mineral assemblage present within Type-1 calc-silicate rock is actinolite + diopside + calcite + quartz + sphene ± microcline ± plagioclase feldspar (andesine to labradorite variety) ± biotite ± epidote ± chlorite, whereas Type-2 is composed of hornblende + garnet + quartz + plagioclase feldspar (anorthite) + calcite + muscovite + chlorite + sphene + epidote. Both the types contain minor proportion of zircon and opaques. Actinolites within the Type -1 calc-silicate rock occur as rhombic to pseudo-hexagonal shape needles with beads or strands like appearance (Fig. 4b). The average crystal length of actinolite needles ranges from 0.45 to 1.1 cm. Actinolites predominantly occur as poikiloblasts within the medium to coarse grained ground mass comprising of calcite, diopside, sphene, microcline, plagioclase feldspar and quartz. Biotite, chlorite and epidote lie in subordinate proportions (Fig. 4c). The variety of biotite exhibit phlogopite mica. Type-2 calc-

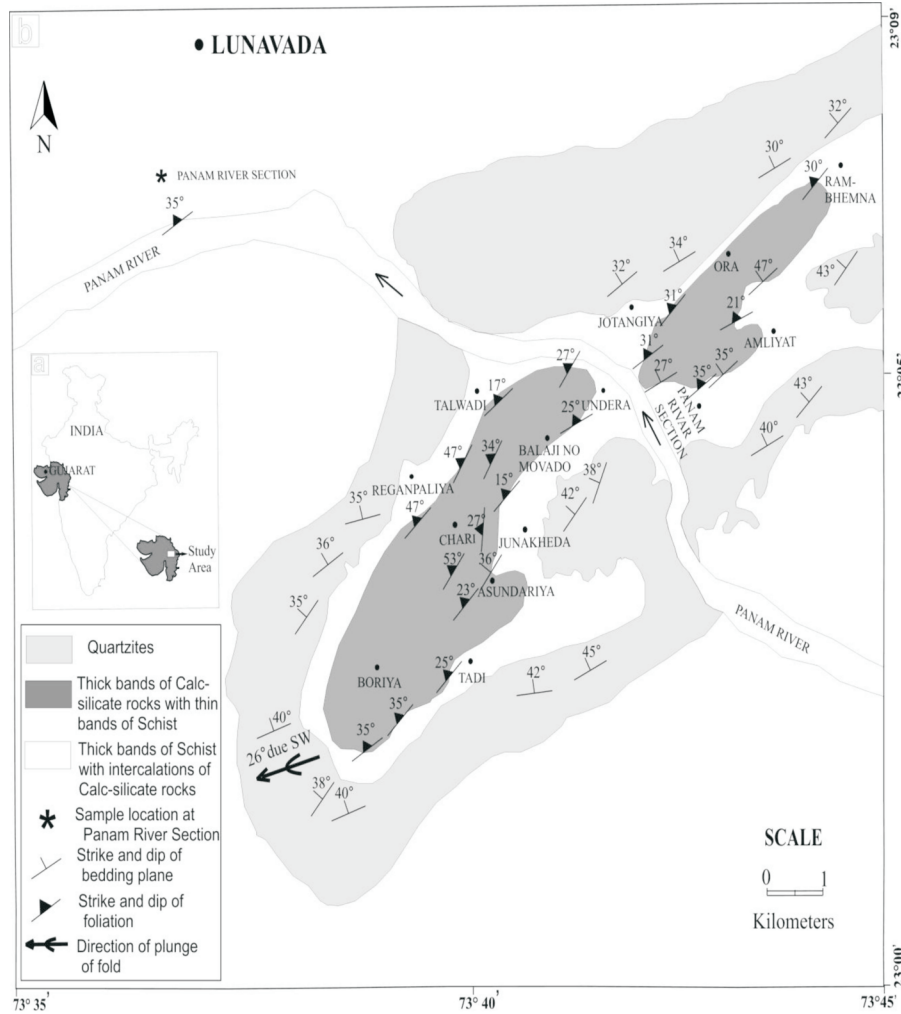


Fig.2. a) Location map; b) Geological map of the study area.



Fig.3. a) Field photograph showing maculose structure on the upper surface of calc-silicate rocks, Loc. Jotangiya; b) Arrow headed fold developed within quartz vein intruding calc-silicate rock indicating synchronous deformation with granite, Loc. Chari; c) Thick granite-pegmatite vein depicting discordant relationship with calc-silicate rocks, Loc. Ora; d) Randomly oriented hornblende laths within Type-2 calc-silicate rocks, Loc. right bank of Panam river.

silicate show subidioblastic grains of hornblende ranging from 0.25 to 0.4cm in length with almandine garnets as skeletal growth (Fig. 4d). Few garnets show partial chloritisation in varied proportions from rim to core (Fig. 4e). The groundmass of this variety is composed of quartz, calcite, microcline and plagioclase feldspar to develop prominent granoblastic polygonal texture with grain boundaries meeting at triple point having approximate 120° angle between them (Fig. 4f). Plagioclase feldspar occurs between 20-30% as fine to medium sized tabular subidioblastic grains. Other Ca-bearing minerals such as calcite, sphene and epidote are present in very less quantity, *i.e.* about 4-15%. Rounded to sub-rounded zircons are present in trace amounts as inclusions in hornblendes and muscovites. Based on the overall texture within two types of calc-silicates, the over printing relationship can be established. The poikiloblasts of actinolite/hornblende and garnet from both the varieties show inclusions of quartz, biotite/muscovite and zircons suggest concordant relationship with the ground mass fabric (Fig. 4g).

Discussion

It is evident from the field relationship that the calc-silicate rocks of Type-1 variety lay in vicinity to the granitic intrusion show typical contact metamorphic structure. The actinolite mineral development within this variety show coarser grain size along with the random orientation of crystals. The Type-2 calc-silicate rocks located at a considerable distance from the granite pluton possess similar character with finer crystal size distributions of hornblende laths. Petrographic analyses reveal that both the types of calc-silicate rocks exhibit identical inclusion trails as compared to the external fabric of the ground mass. The acquired results imply that the development of actinolites and hornblendes are the product of late stage of metamorphic crystallisation. In other words progressive regional metamorphic condition had no control over the development of these minerals.

Microstructural analysis proposed by Mamtani *et al.* (2001) established a time relationship between metamorphism and deformation based on the inherent porphyroblast-matrix relationships within metapelites of the region. Their inferences suggest progressive regional metamorphic mineral growth co-relatable with the respective deformation events are chlorite + muscovite during D_1 , whereas biotite + garnet till syn-late D_2 event. D_3 event do not support any new mineral growth hence it was devoid of any metamorphism. In all, two phases of metamorphism has been recorded *viz.*, M_1 and M_2 . M_1 indicate progressive regional metamorphism, whereas M_2 has partial retrogressive signatures during late D_2 event. Such signatures have been shown by the development of chlorite along fractures within syn- D_2 garnets. D_3 deformation event was characterised by syn-tectonic granite emplacement which gave rise to the thermal metamorphism in terms of grain coarsening. Crystal Size Distribution studies (CSDs) on

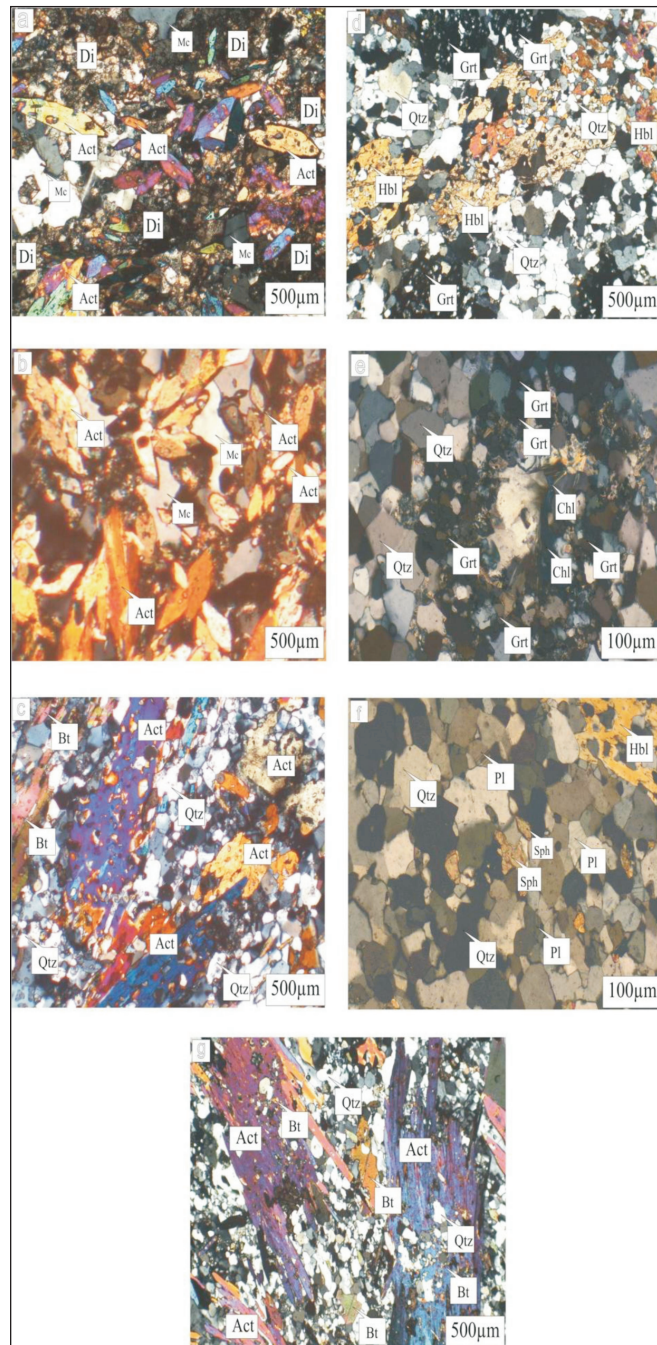


Fig.4. Photomicrographs of calc-silicate rocks in crossed polars showing a) Hornfelsic texture within Type-1 calc-silicate rocks; b) Rhombic to pseudo-hexagonal shaped actinolites with beads or strands like appearance; c) Poikiloblasts of actinolites; d) Skeletal texture shown by hornblendes and garnets; e) Partial chloritization shown by garnet grain from rim to core; f) Quartz and plagioclase feldspar grains unite to form granoblastic polygonal texture; g) Concordant relationship of internal fabric with the ground mass.

schists and quartzites of Lunavada region indicate strong effect of annealing due to static re-crystallisation over quartz grain and development of granoblastic microstructure in quartzites, present nearer to the granitic intrusion (Mamtani and Karanth, 1996). However, field evidences of discordant granite pegmatite in the southern part of the study area indicate it's prolong emplacement record.

Conclusion

Based on the above evidences from Type-1 and Type-2 calc-silicate rocks the present work proposes a slight refinement within the time relationship between metamorphism and deformation in Proterozoic rocks of the Lunavada region. The salient findings of the study has been summarised in (Table 2). The D_3 phase of deformation coeval with granite emplacement supports new mineral growth due to thermal metamorphism. These mineral includes actinolites within Type-1 and hornblendes in Type-2 along with sphene, plagioclase feldspar and epidote in both the varieties.

Minerals	Deformational events		
	D_1 ↓ M_1	D_2 ↓ M_{2-1} and M_{2-2}	D_3 and syn to post D_3 phase followed by thermal event along with static recrystallization
Chlorite (1)	←→		←→
Chlorite (2)			←→
Biotite (1)	←→		
Biotite (2)		←→	
Garnet		←→	
Muscovite	←→		←→
Quartz	←→		←→
Act/Hbl			←→
Sphene			←→
Plagioclase-feldspar			←→
Epidote			←→

Table 2: Development of new minerals (bold font) in calc-silicate rocks in response to the syn-post D_3 granite emplacement (*modified after* Mamtani *et al.*, 2001).

Acknowledgements

The authors are grateful to Prof. L.S. Chamyal, Head, Department of Geology, M.S. University of Baroda, Vadodara for providing necessary facilities. First author acknowledge the help rendered by Ms. Apurva and Ms. Mitali during introductory field work.

References

- Joshi, A.U., Limaye, M.A. and Deota, B.S. (2016). Microstructural indicators of post-deformational brittle-ductile shear zones, Lunavada region, Southern Aravalli Mountain Belt, Gujarat, India. *Jour. M.S.U.S.T.*, v. 51(1), pp. 19-27.
- Gopalan, K., Trivedi, J.R., Merh, S.S., Patel, P.P. and Patel, S.G. (1979). Rb-Sr age of Godhra and related granites, Gujarat (India). *Proc. Indian Acad. Sci. (Earth & Planet. Sci.)*, v. 88A, pp. 7-17.
- Gupta, S.N., Arora, Y.K., Mathur, R.K., Iqbaluddin, B.P., Sahai, T.N. and Sharma, S.B. (1995). Geological map of the Precambrians of Aravalli Region, Southern Rajasthan and Northeastern Gujarat, India. *Geol. Surv. India Publ.*, Hyderabad.
- Gupta, S.N., Arora, Y.K., Mathur, R.K., Iqbaluddin, B.P., Sahai, T.N. and Sharma, S.B. (1980). Lithostratigraphic map of Aravalli Region, Southern Rajasthan and North Eastern Gujarat. *Geol. Surv. India Publ.*, Hyderabad.
- Gupta, S.N., Arora, Y.K., Mathur, R.K., Iqbaluddin, B.P., Sahai, T.N. and Sharma, S.B. (1997). The Precambrian geology of the Aravalli region, Southern Rajasthan and Northeastern Gujarat. *Mem. Geol. Surv. India*, v. 123, pp. 58-65.
- Gupta, S.N., Mathur, R.K. and Arora, Y.K. (1992). Lithostratigraphy of Proterozoic rocks of Rajasthan and Gujarat. *Rec. Geol. Surv. India*, v. 115, pp. 63-85.
- Iqbaluddin, B.P. (1989). Geology of Kadana reservoir Area, Panchmahals district, Gujarat and Banswara and Dungarpur districts, Rajasthan. *Mem. Geol. Surv. India*, v. 121, 84p.
- Mamtani, M.A. (1998). Deformational mechanisms of the Lunavada Pre-Cambrian rocks, Panchmahal district, Gujarat. Unpubl. Ph.D. thesis, M.S. University of Baroda, 268p.
- Mamtani, M.A. and Greiling, R.O. (2005). Granite emplacement and its relation with regional deformation in the Aravalli Mountain Belt (India) - inferences from magnetic fabric. *Jour. Struct. Geol.*, v. 27, pp. 2008-2029.
- Mamtani, M.A., Greiling, R.O., Karanth, R.V. and Merh, S.S. (1999). Orogenic deformation and its relation with AMS fabric - an Example from the Southern Aravalli Mountain Belt, India. In: Radhakrishna, T. and Piper, J.D. (eds.), *The Indian Subcontinent and Gondwana: A Palaeomagnetic and Rock Magnetic Perspective*. *Mem. Geol. Soc. India*, v. 44, pp. 9-24.
- Mamtani, M.A. and Karanth, R.V. (1996). Effect of heat on crystal size distributions of quartz. *Curr. Sci.*, v. 70, pp. 396-399.
- Mamtani, M.A., Karanth, R.V., Merh, S.S. and Greiling, R.O. (2000). Tectonic evolution of the Southern part of Aravalli Mountain Belt and its environs- possible causes and time constraints. *Gond. Res.*, v.3, pp. 175-187.
- Mamtani, M.A., Merh, S.S., Karanth, R.V. and Greiling, R.O. (2001). Time relationship between metamorphism and deformation in the Proterozoic rocks of Lunavada region, southern Aravalli Mountain Belt (India) - a microstructural study. *Jour. Asian Earth Sci.*, v. 19, pp. 195-205.
- Mamtani, M.A., Karmakar, I.B. and Merh, S.S. (2002). Evidence of

polyphase deformation in gneissic rocks around Devgadhi Bariya: implications for evolution of Godhra granite in the Southern Aravalli region (India) *Gond. Res.*, v. 5(2), pp. 401-408.

Sen, K. and Mamtani, M.A. (2006). Magnetic fabric, shape preferred orientation and regional strain in granitic rocks. *Jour. Struct. Geol.*, v. 28, pp. 1870-1882.